Production of green fuels using novel catalyst via Fischer-Tropsch synthesis:
catalyst preparation and characterisation of iron and cobalt on calcium support

By

Ahmad Fikry bin Mohd Anwar

Dissertation submitted in partial fulfilment of

the requirement for the

Bachelor of Engineering (Hons)

(Chemical Engineering)

January 2013

Universiti Teknologi PETRONAS
Bandar Seri Iskandar
31750 Tronoh
Perak Darul Ridzuan

CERTIFICATION OF APPROVAL

Production of green fuels using novel catalyst via Fischer-Tropsch synthesis: catalyst preparation and characterisation of iron and cobalt on calcium support

by

Ahmad Fikry bin Mohd Anwar

A project dissertation submitted to the
Chemical Engineering Programme
Universiti Teknologi PETRONAS in partial
fulfilment of the requirement for the
BACHELOR OF ENGINEERING (Hons)
(CHEMICAL ENGINEERING)

Approved by,

(Dr. Bawadi b. Abdullah)

UNIVERSITI TEKNOLOGI PETRONAS

TRONOH, PERAK

January 2013

CERTIFICATION OF ORIGINALITY

This is to certify that I am responsible for the work submitted in this project, that the original work is my own except as specified in the references and acknowledgements, and that the original work contained herein have not been undertaken or done by unspecified sources or persons.

(AHMAD FIKRY BIN MOHD ANWAR)

ABSTRACT

Fischer-Tropsch (FT) synthesis is a process where syngas is converted into larger hydrocarbon structure. The process had played an important role after the rise of the petroleum price and the current outlook of the global oil and gas resources. In Malaysia, FT technology was implemented as early from 1993 by Shell Gas in Bintulu. The current studies of the FT synthesis cover a wide range of catalyst support, but limestone was not yet tested as the one of them. The prospect of this study is to see the suitability of calcium-based catalyst loaded with common metal catalyst used in FT technology (Fe and Co) to see the rate of conversion in term of its effectiveness with reference to CaO and its capacity as catalyst support. The catalyst will be prepared using precipitation method and had been analyzed with TGA, XRD, BET, TEM, FESEM and TPR/TPO. From overall analysis, the CaO provides the best result from BET, while from XRD, TEM and FESEM it can be notified that the catalyst has carbon deposition, water deposition and traces of sulphur for Co/CaO. The scopes of the objectives are achieved and the experiment should proceed to part B, which is the Fischer-Tropsch synthesis of the catalysts.

ACKNOWLEDGEMENT

I would like to express my sincerest gratitude to the following persons

- My supervisor, Dr. Bawadi b. Abdullah for the exposure on the Fischer-Tropsch topic and for the guidance and help over the project period
- My dear lecturer, Prof. Dr. Yoshimitsu Uemura who had given me brief outlines for the catalyst preparation and characterization
- The lab technicians for their support and their assistance throughout the project period
- The Universiti Teknologi PETRONAS (UTP) Chemical Engineering Department and the Central Analytical Lab (CAL) in UTP who had provided a good exposure for research-based project in my undergraduate years

Finally, I dedicate this work to my dear family and friends, who are there when I needed them the most – especially my parents – who had fueled me to see ends to ends.

Table of Content

Table of Figures

List of Tables

Abbreviations and Nomenclatures

FT	Fischer-Tropsch
FTS	Fischer-Tropsch synthesis
HTFT	High Temperature FT
LTFT	Low Temperature FT
GTL	Gas-to-Liquid
WGS	Water-Gas-shift
BET	Brunauer-Emmett-Teller
BJH	Barret-Joyner-Halenda
SP	Single Point
FESEM	Field Emission Scanning Electron Microscope
TEM	Transmission Electron Microscope
XRD	X-ray Diffraction
GC	Gas chromatography
FID	Flame ionisation detector
TGA	Thermogravimetric analysis
TPR	Temperature programmed reduction
TPO	Temperature programmed oxidation
Adsp	Adsorption
Dsrp	Desorption
Avg	Average
Å	Angstrom
m	Metre
nm	Nanometre
μ	Micro
g	Gram
wt%	weight percent
ml	Millilitre
K	Kelvin
e	Error
M1	degradation ratio catalyst support
M2	degradation ratio metal oxide
Fe	Iron
Co	Cobalt
Ca	Calcium
Ni	Nickel
Ru	Ruthenium
$CaCO_3$	Calcium Carbonate
CaO	Calcium Oxide
CO_2	Carbon Dioxide
CO	Carbon Monoxide
H_2	Hydrogen
H_2O	Water
Fe_2O_3	Iron (III) Oxide

CoO	Cobalt (II) Oxide
Fe(NO3)3.9H2O	Iron (III) Nitrate hydrates
CoSO4.H2O	Cobalt (II) sulphate hydrates
Fe/CaO	Iron on calcium oxide support
Co/CaO	Cobalt on calcium oxide support

CHAPTER 1

1 INTRODUCTION

1.1. Problem Statement

In current research of Fischer-Tropsch (FT) reaction, calcium is usually used as a promoter for the catalyst reaction. In Malaysia, the FT synthesis is being done in Shell Bintulu plant to convert synthetic gas into high-value synthetic paraffin.

With the abundant availability of limestone all around Malaysia – which consists of calcium mainly and traces of magnesium – this has provide a valid questioning of whether the limestone can be used as a catalyst support for the FT synthesis. This research is aimed to see whether calcium can provide a significant conversion of the syngas with iron and cobalt as the catalyst loading.

1.2 Objectives

− To study the catalyst characterization of calcium-based catalyst loaded with iron (Fe) and cobalt (Co) respectively.

1.3 Scope and limitations of the study

− To prepare the calcium –based catalyst loaded with 5 weight percent of iron and cobalt via precipitation method.
− To study the thermal decomposition of calcium carbonate ($CaCO_3$) for calcination of the catalysts.
− To study the chemical composition of the catalyst before and after the calcination.
− To study the pore volume of the catalysts.
− To study the activation temperature for each catalysts.
− To study the surface morphology and the metal deposition on calcium-based catalyst

CHAPTER 2

2   LITERATURE REVIEW

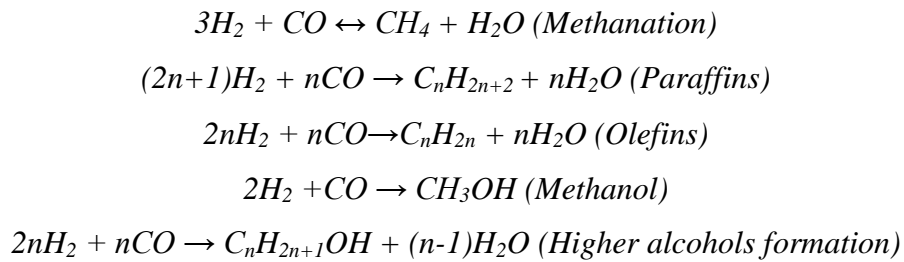### 2.1 History of Fischer-Tropsch synthesis

The development of Fischer-Tropsch (FT) technology can be noted from the earlier development of Carl Bosch and Friedrich Bergius that won Nobel Prize for Chemistry in 1931 for the recognition of their invention and development of chemical high pressure method. The process is similar in term of the resources used in these processes – converting coal into petroleum. Bergius steps required the coal to be crushed and dissolved in heavy oil to form a paste. The paste was brought to react with hydrogen as at high temperature (around 200 atmospheres) and at high temperature (around 673K) to obtain petroleum-like liquids. The differences between these two processes that is FT reacted under near and intermediate atmospheric pressure (around 1-10 atmospheres) with mild temperature (around 453K to 473K) to convert a mixture of carbon monoxide and hydrogen (or usually called as syngas) from a reaction between coal and steam to form petroleum-like liquid. The development of the technology were fueled by two factors; Germany increased dependency on gasoline and diesel oil engines, and the urbanization, industrialization of Germany that led the country to seek for better fuel like petroleum that provides more energy compared to coal. (Stranges, 2007)

The FT process can also be divided into two – the High Temperature Fischer Tropsch (HTFT) which are operating at 603-623K and Low Temperature Fischer Tropsch (LTFT) which usually ranging from 453-523K.

The FT process aimed to have a catalytic conversion from syngas to hydrocarbons over a catalyst. The reactions can be simplified and expressed as (Luo & Davis, 2003) stated:

$$(2n+1)H_2 + nCO \rightarrow C_nH_{2n+2} + nH_2O$$
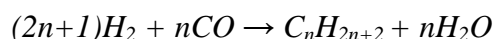
In details, the FT process can be divided into three parts: product forming reactions, non-product forming reactions and secondary reaction (Motchelaho, 2011). The product forming reactions are methanation, paraffins, olefins, methanol and higher alcohols reactions.

$$3H_2 + CO \leftrightarrow CH_4 + H_2O \text{ (Methanation)}$$

$$(2n+1)H_2 + nCO \rightarrow C_nH_{2n+2} + nH_2O \text{ (Paraffins)}$$

$$2nH_2 + nCO \rightarrow C_nH_{2n} + nH_2O \text{ (Olefins)}$$

$$2H_2 + CO \rightarrow CH_3OH \text{ (Methanol)}$$

$$2nH_2 + nCO \rightarrow C_nH_{2n+1}OH + (n-1)H_2O \text{ (Higher alcohols formation)}$$

The non-product forming are the Boudouard reaction, carbide formation, catalyst oxidation and catalyst reduction from the carbon monoxide and water compound.

$$2CO \rightarrow C + CO_2 \text{ (Boudouard reaction)}$$

$$xM + 2CO \rightarrow M_xC + CO_2 \; ; \; xM + CO + H_2 \rightarrow M_xC + H_2O \text{ (carbide formations)}$$

$$xM + yH2O \rightarrow M_xO_y + yH_2 \text{ (catalyst oxidation)}$$

$$M_xO_y + yCO \leftrightarrow xM + yCO_2 \text{ (catalyst reduction)}$$
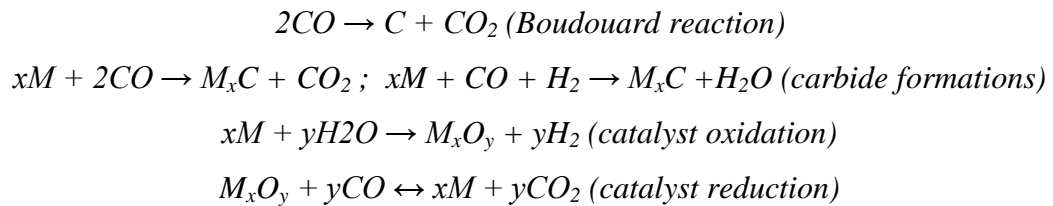
The secondary reaction that happens in FT process is the water-gas-shift (WGS) reaction that occurs in the process.

$$CO + H_2O \leftrightarrow CO_2 + H_2 \text{ (WGS reaction)}$$

As for Malaysia, the FT processes were used in Shell Bintulu plant as early from 1993. However, the process was adapted to fit from Gas to Liquid processes (GTL). The difference is that the source of carbon monoxide and hydrogen (syngas) are from methane and oxygen (Hoek, 2006). The plant was initially has the capa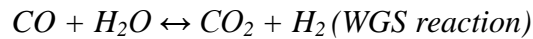city to produce 12, 500 barrel per day but in present after plant extension, it was able to produce around 14, 600 barrel per day (Rapier, 2010).

Being dubbed as clean energy and very pure fuel, the FT fuel needs to be used in blends. This is due to the lack of aromatic compounds that can act as a lubricant and help to swell rubber seals to prevent leakage in fuel system (HubPages).

2.2 Fischer-Tropsch Catalyst

The scope of this project is to use limestone-based catalyst loaded with common catalyst used in Fischer-Tropsch synthesis (for example iron and cobalt) to study the effectiveness and the yield as compared to other catalyst base.

The primary reason is due to the nature that limestone is readily available and abundant in Malaysia geographical view. Consisted of mainly mineral calcite, these rocks are mainly available in Klang Valley, Kinta Valley, Kedah-Perlis (including Langkawi Islands) Kelantan and Pahang in Peninsular Malaysia (Tan, 2002). The main interest here is that limestone is a sedimentary rock dissociated only under high temperature around 1171K (with basis of pure compound) (Lime).

The choice for the catalyst loading in limestone is based on the common catalyst being used in the industry. This includes Fe, Co and Ru as they provide the best possibilities for the hydrogenation of carbon monoxide in FT synthesis. The presence of Ru is flexible as promoters for Co catalyst as it enhanced the initial reduction and in-situ regeneration of the catalyst. Ru also helps to keep the catalyst surface 'clean'. As for itself, Ru is a very active catalyst for FT synthesis and very versatile. At high temperature it highly active for methanation sites catalyst while at lower temperature it produces a huge amount of waxes in low polyethylene range that the selectivity can controlled by the pressure inside the reactor. There are also concerns on catalyst poisoning and catalyst deactivation for the whole synthesis reaction (Dry, 2004)

It can also be noted that there are no significant catalyst deactivation occurred for Co-based catalyst from 453-473K and mild deactivation only occurring from 483-493K (Yao, 2011). From the thesis, it can be summarized that Fe-based catalyst at HTFT will produce gasoline or linear low molecular mass olefins as compared to LTFT that will produce high molecular mass linear wax. Co-based catalyst is ensured to have WGS reaction, while having higher selectivity and activity for linear paraffins conversion. However, Co-based catalyst is more prone to deactivate as well as poisoned as compared to Fe-based catalyst. As for catalyst promoters, Ni, Ru and Co is mostly used to increase the conversion of CO_2 into hydrocarbons commercially.

2.3 Reactor

The main concern for FT reactor choice is the ability to rapidly remove heat from the catalyst particles to avoid overheating. Otherwise, there would be high chances of the increase of rate of deactivation due to sintering and fouling and undesirable amount of methane. The options are to force the syngas in high linear velocities through long narrow tubes packed with catalyst particles to achieve turbulent flow or to conduct the synthesis in fluidized bed catalyst reactor. However, in term of poisoning, fluidized bed is more risky as the poison enters the system; the whole catalyst would be rendered useless as compared to fixed bed since only the top layer is deactivated. As currently, there are two operating conditions for FT synthesis. There are High Temperature FT (HTFT) and Low Temperature FT (LTFT). The HTFT operated around 573-623K and commonly used to produce gasoline and linear low molecular mass olefins. While for LTFT usually operated from 473-513K to produce high molecular mass linear waxes (Dry, Catalysis Today 71, 2002)

Figure 2.1 shows the summary of the reactors used in the FT synthesis.
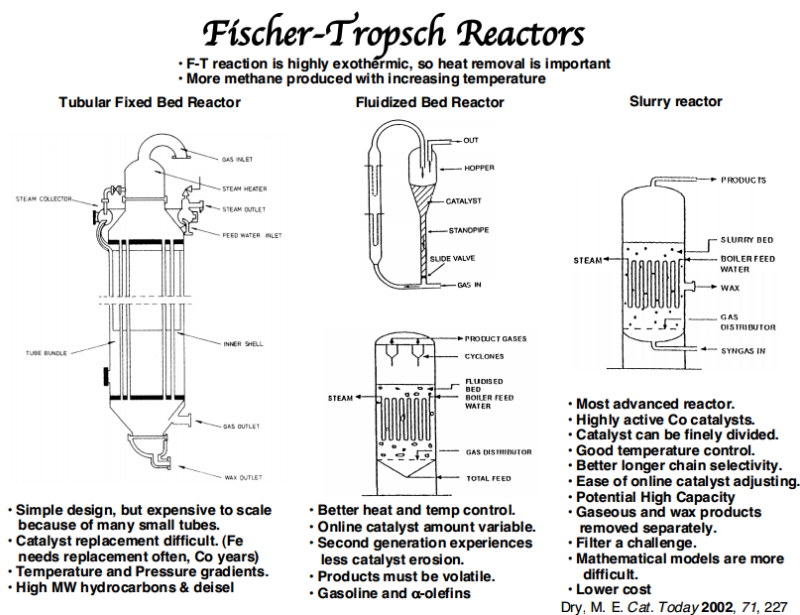

Figure 2.1: The summary of reactors used in FT synthesis[11]

For this experiment, the reactor setup and components are as follows:
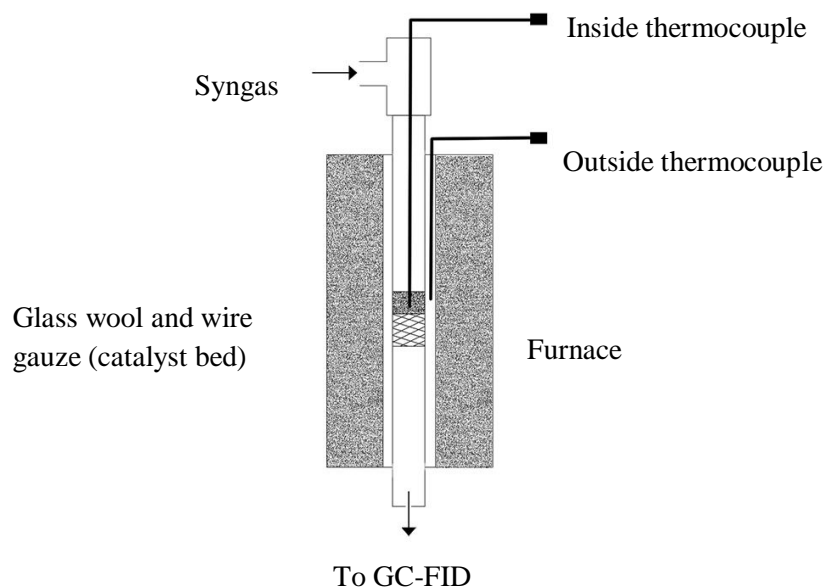

Figure 2.2: Reactor setup for Fischer-Tropsch synthesis

The reactor used for this experiment is a single tubular fixed bed reactor. In order to maintain safety of the experiment environment, the reactor setup will be arranged inside a gas chamber.

CHAPTER 3

3 Methodology

3.1 Part A: Catalyst characterization and preparation

3.1.1 Thermal degradation of calcium carbonate (CaCO3)

1. A sample of calcium carbonate (10μg) is put under Thermogravimetric Analyzer (TGA) to obtain the thermal degradation curve of calcium carbonate; which will be used as a reference for calcinations of calcium carbonate. The reaction would be from calcium carbonate to calcium oxide with carbon dioxide gas:

   $CaCO_3 \rightarrow CaO + CO2$

2. The sample would be heated up to 1173K with the increment of 10K/minute. The sample would then be heated for 30 minutes at the maximum temperature to ensure all of the samples are converted into CaO.

3. The thermal profile of the sample is obtained containing the decomposition curve and the temperature curve of the analysis.

4. A 50g samples of CaO is prepared in the oven using the thermal curve as a reference (i.e.: drying at 1123K for overnight)

3.1.2 Chemical composition and surface adsorption

1. A part of the sample of $CaCO_3$ and CaO are prepared for the x-ray diffraction (XRD) method to determine the chemical composition of both compounds as a reference after the impregnation method.

2. Another part of both of the compound are taken for the BET surface adsorption analysis.

3. Based on the analysis of the BET, the sample with highest pore volume and specific surface area are taken for the incipient wetness impregnation method.

3.1.3   Incipient wetness impregnation

1. The desired amount of catalyst loading is 5 wt% of cobalt and iron – respectively of both metals. The volumes of the metal solutions are respectively to the pore volume obtained in BET analysis. Approximately 30 grams of Ca samples are used for each respective loading.

2. The samples are placed in a beaker containing a specified amount of metal solutions with specific concentration to obtain the required catalyst loading.

3. The catalysts are then dried in the oven for overnight on 363K and are labeled respectively to the loading and type of metal.

3.1.4   Surface analysis of impregnated catalyst

1. Each of the catalysts is taken for Field Emission Scanning Electron Microscope (FESEM) and Transmission Electron Microscope (TEM) to see the morphology and the dispersion of the metal site on the catalyst.

3.1.5   Chemical composition of impregnated catalyst

1. Each of the samples is taken for another XRD method to determine the composition of the catalyst after the loading and also to determine the presence of crystallinity in the catalysts by observing sharp peaks.

2. The graphs are compared with the XRD results before the impregnation method to determine the composition of the catalysts.
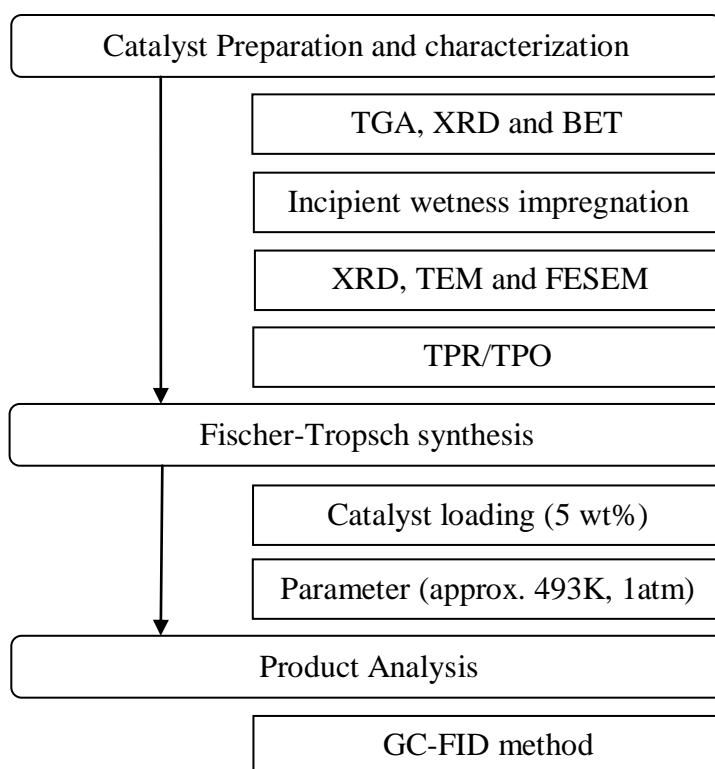
3.2   Part B: Fischer-Tropsch Synthesis (FTS)

1. The reactor is set for the experiment at atmospheric pressure. The furnace temperature is set up to be in 493 Kelvin

2. The flow of the syngas is controlled so that the amount of syngas could be maintained.

3. After some time, the product gases are taken with a gas syringe for analysis.

4. The synthesis is repeated for data optimization and is repeated with another catalyst loading.

3.2.1 Gas product analysis

Samples of the gas products are taken with gas syringe to analyze using gas chromatography method with flame ionization detector (GC-FID) to determine the composition of the gas samples.

### 3.3 General overview methodology of the study

```
┌────────────────────────────────────────────────┐
│      Catalyst Preparation and characterization  │
└────────────────────────────────────────────────┘
        │            ┌────────────────────────────┐
        │            │      TGA, XRD and BET       │
        │            └────────────────────────────┘
        │            ┌────────────────────────────┐
        │            │  Incipient wetness impregnation │
        │            └────────────────────────────┘
        │            ┌────────────────────────────┐
        │            │    XRD, TEM and FESEM       │
        │            └────────────────────────────┘
        │            ┌────────────────────────────┐
        │            │          TPR/TPO            │
        ▼            └────────────────────────────┘
┌────────────────────────────────────────────────┐
│            Fischer-Tropsch synthesis            │
└────────────────────────────────────────────────┘
        │            ┌────────────────────────────┐
        │            │    Catalyst loading (5 wt%) │
        │            └────────────────────────────┘
        │            ┌────────────────────────────┐
        │            │  Parameter (approx. 493K, 1atm) │
        ▼            └────────────────────────────┘
┌────────────────────────────────────────────────┐
│                Product Analysis                 │
└────────────────────────────────────────────────┘
                     ┌────────────────────────────┐
                     │        GC-FID method        │
                     └────────────────────────────┘
```

CHAPTER 4

4   Results and Discussion

  4.1   Thermal decomposition of Calcium Carbonate (TGA)

The maximum temperature set is 1173K and the temperature ramp is 10K/minute. The graph below shows the thermal decomposition profile of $CaCO_3$.

Decomposition of $CaCO_3$ is expected to be from the following chemical reaction:

$$CaCO_3 \rightarrow CaO + CO_2$$
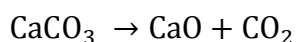
In which, calcium carbonate decompose in heat to produce calcium oxide and carbon dioxide. The CaO is relatively stable in normal condition (289K, atmospheric pressure) but it reacts with water to form limewater and it readily absorbs CO_2 from the environment over time (based from the CaO Material Safety Datasheet).
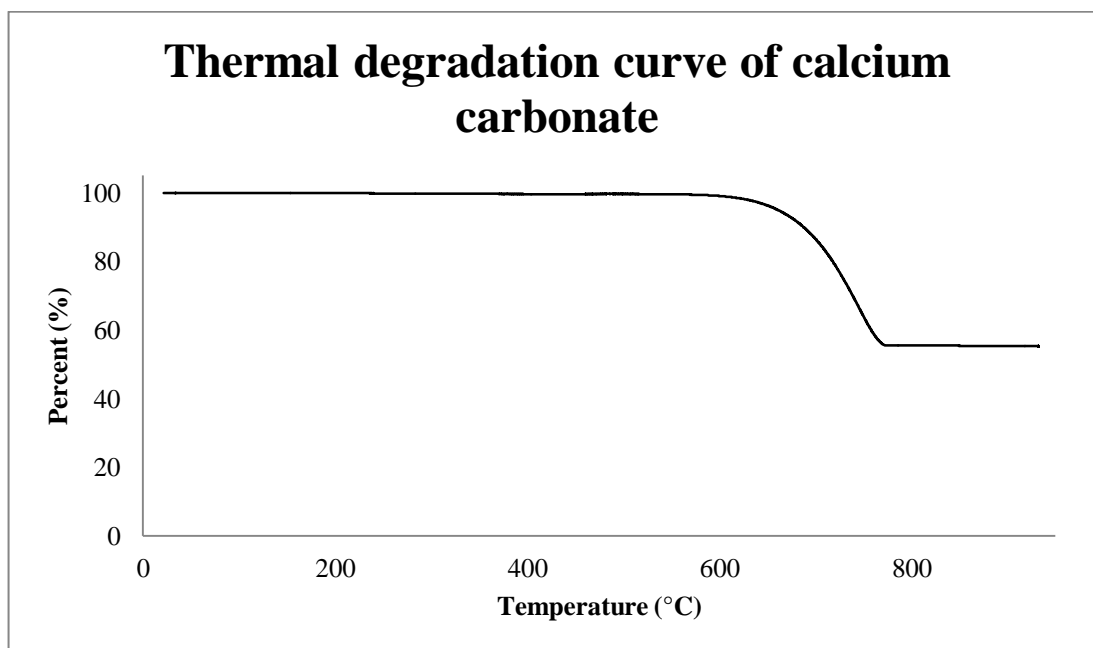
Figure 4.1: Thermal decomposition of Calcium Carbonate

From the graph, the decomposition starts approximately at 873K and the $CaCO_3$ decomposed almost completely at more than 1023K.

The decomposition of $CaCO_3$ will give approximate temperature for the calcination to obtain a heterogeneous calcium-based catalyst with metal support from precipitation method.

The TGA also will provide the data of the decomposition ratio of $CaCO_3$ into CaO. The result shown that the TGA decomposition ratio is 0.5518 while the theoretical decomposition ratio is 0.5603. The difference error is around 1.5%. This error might come from the presence of water contaminant in the sample.

4.2   Precipitation method and calcination

The catalysts are prepared from the mole calculation and with the basis that the metal loads will be 5 weight percent of the catalyst weight. The expected weight of Fe loaded catalyst is 50g after calcination and Co loaded catalyst 30g after calcination. Therefore, Fe is expected to be around 2.5g while Co is expected to be around 1.5g. The table below shows the calculation on how the mass of the salt are determined.

Fe loaded catalyst		Co loaded catalyst	
Mol	Mass (g)	mol	Mass (g)
0.04476	2.5	0.025454	1.5
Calcium weight			
Mol	Mass (g)	mol	Mass (g)
1.1851297	47.5	0.711078	28.5

Component	Mass (g)	Component	Mass (g)
$CaCO_3$	118.61964	$CaCO_3$	71.17178
$Fe(NO_3)_3 . 9H_2O$	18.08415	$CoSO_4 . H_2O$	4.403784

Table 4.1: Catalyst mass calculation

The metal salts are dissolved in water at 150 ml for Fe and 100 ml for Co catalyst. It is heated under moderate temperature and the $CaCO_3$ are added to the solution. It was stirred continuously with magnetic stirrer at moderate speed until almost all the water evaporated. The slurry mixtures are then filtered and dried in an oven at 363K overnight. The dried catalyst are then crushed and weighed for the calcination process.

In the calcination, the reduced reactions considered are as follows:

$$CaCO_3 \rightarrow CaO + CO_2$$

$$Fe(NO_3)_3 . 9H_2O \rightarrow NO_2 + 9H_2O + Fe_2O_3$$

$$CoSO_4 . H_2O \rightarrow SO_3 + H_2O + CoO$$
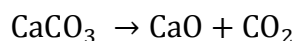
From these reactions, the ratio of decomposition can be easily obtained from the mass ratio of the molar mass of the decomposed with the initial molar mass. These data will be used as the theoretical decomposition ratio of each of the component.

Compound	Notation	Theoretical ratio	TGA ratio
$CaCO_3$	CaO	0.5603	0.5518
$Fe(NO_3)_3 . 9H_2O$	Fe	0.3953	-
$CoSO_4 . H_2O$	Co	0.4331	-

Table 4.2: Theoretical decomposition ratio of each catalyst sample (calculation are included in appendix A)

Using a mass balance principle, the decomposition of both catalysts loaded with metal oxides are as follows:

$$Total\ decomposition\ ratio = 0.95 \times M_1 + 0.05 \times M_2$$

Where M_1 is the ratio for the catalyst support and M_2 is the ratio for the metal oxide.

Hence,

Fe/CaO: $\qquad 0.95 \times 0.5603 + 0.05 \times 0.3953 = 0.55205$

Co/CaO: $\qquad 0.95 \times 0.5603 + 0.05 \times 0.4331 = 0.55394$

The mass was recorded and tabulated for the experiment procedures (note: the catalysts are noted by their desired final composition).

	CaO	Fe/CaO	Co/CaO
Crucible Mass (g)	61.1572	56.0857	56.8943
Mass sample before (g)	50.0006	50.0171	30.0095
Mass sample after with crucible (g)	91.8112	84.6264	74.593
Mass sample after (g)	30.654	28.5407	17.6987
Decomposition ratio	0.6131	0.5706	0.5898

Table 4.3: Experimental decomposition ratio of each catalyst sample

Here the error can be calculated as well as predicting whether the outcome composition is as what it is expected. The error is calculated as below equation:

$$e \, (\%) = \left| \frac{(X_{theoretical} - X_{actual})}{X_{actual}} \right| \times 100$$

	CaO	Fe/CaO	Co/CaO
Theoretical	0.5603	0.55205	0.55394
Experimental	0.6131	0.5706	0.5898
Error (%)	8.6	3.3	6.1

Table 4.4: Percentage error of the decomposition ratio of each catalyst sample

The amount of error present might indicate that the decompositions are not as what being considered earlier. The samples might have a few contaminants present such as water and traces of gases or other elements. The sample composition will be analyzed in X-ray diffraction (XRD) method.

4.3 Chemical composition of catalysts (XRD)

The catalyst samples are taken to the XRD to determine the composition before and after the calcination process. From here and forward, the samples for Fe and Co loading will be denoted by Fe/CaO and Co/CaO respectively.

4.3.1 Before calcination
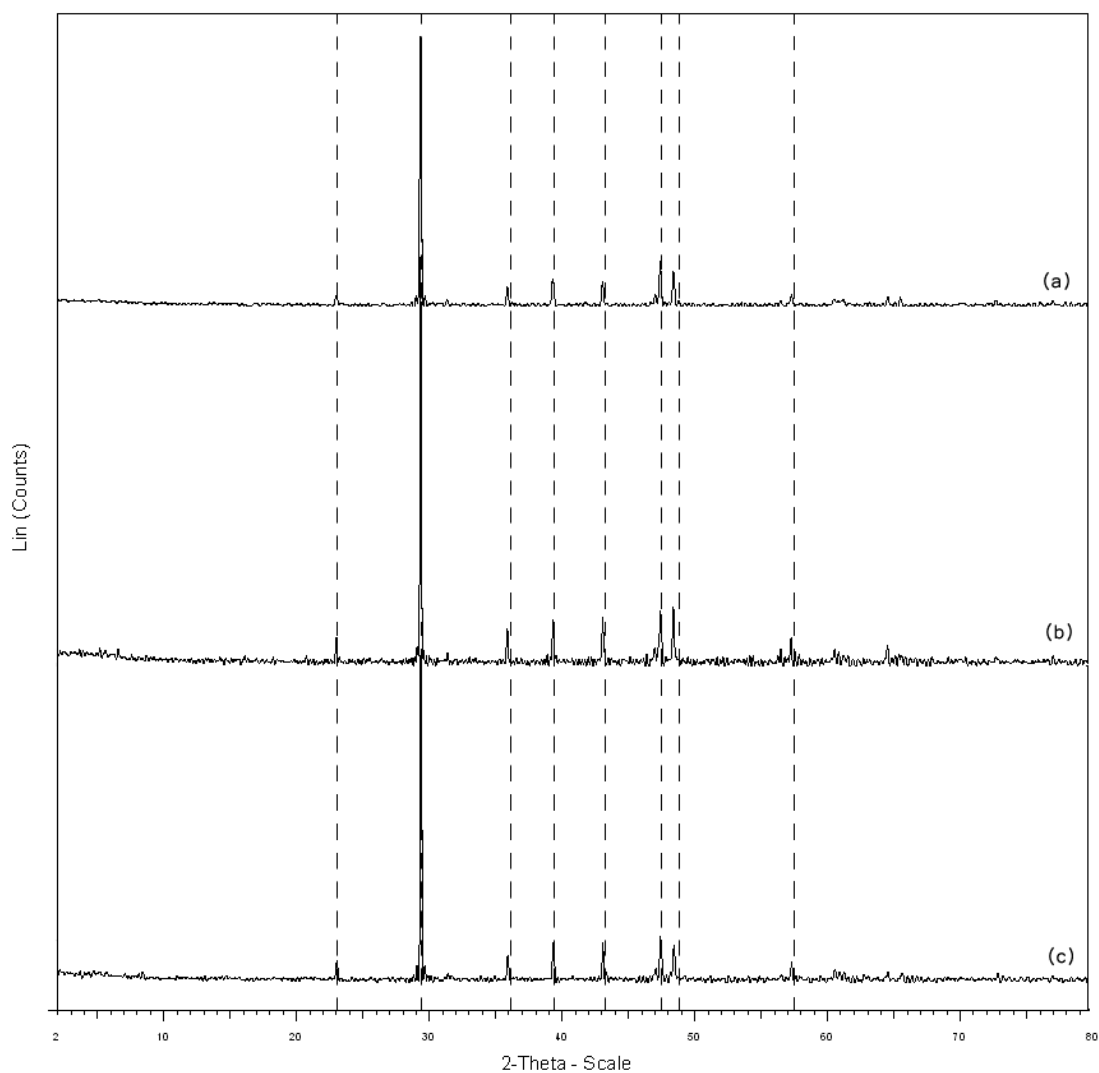
Figure 4.2: XRD diffraction pattern of compounds before calcination; (a) CaO, (b) Fe/CaO and (c) Co/CaO

Figure 4.2 shows the diffraction patterns of the three compounds before the calcination. There is almost no difference in the pattern intensity between the three samples. The samples represent $CaCO_3$ compound and the lack of the peaks difference here might indicate the metal present not as crystalline but as metal hydroxide ($Fe(NO_3)_3 \cdot 9H_2O$ and $CoSO_4 \cdot H_2O$ respectively).

4.3.2 After calcination
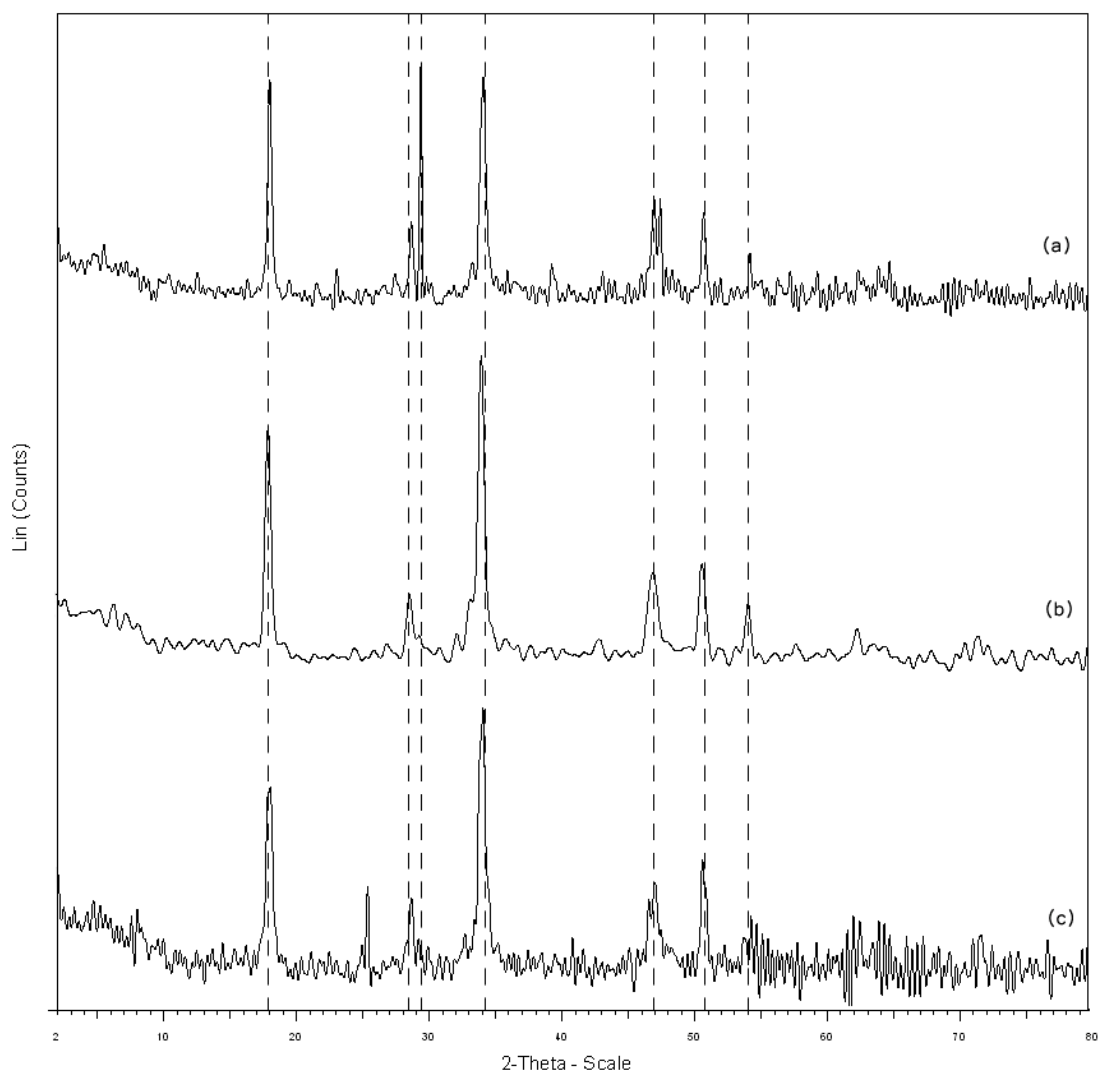
Figure 4.3: XRD diffraction pattern of compounds after calcination; (a) CaO, (b) Fe/CaO and (c) Co/CaO

From figure 4.3, it is shown that the crystalline structure and planes of the atom of the catalyst change after the calcination based on the peak shifts. From here it could be deduced that the samples are mostly presented by the calcium oxide compound. Although, from the databank the compound noted are calcium hydroxide – this is finding is consistent as it is part of the CaO properties. The CaO absorbs the surrounding humidity to form calcium hydroxide. It is noted that the CaO sample still have traces of carbon, in which it may indicate that the calcination process of the calcium carbonate sample are not totally converted into CaO during the calcination. As for the metal oxides present, the peak differences might indicate the presence of metal crystalline that is different from CaO compound.

15

4.4 Surface area of catalysts (BET) and Adsorption isotherm plot

	Surface Area (m²/g)			
	Single-point	BET	Langmuir	t-Plot
CaCO3	1.57	1.91	3.61	3.12
CaO	10.69	11.53	17.76	13.47
Fe/CaO	6.48	6.77	10.07	0.24
Co/CaO	10.14	10.58	15.77	0.23

Table 4.5: Collection of surface area data

Table 4.5 showed that the surface area of the catalysts. It is shown that CaO can provide more surface area as compared to $CaCO_3$. From these tests, it is confirmed that the samples are all mesopores in nature. The following figure is the graph representation of the surface area of the samples based on several analyses.
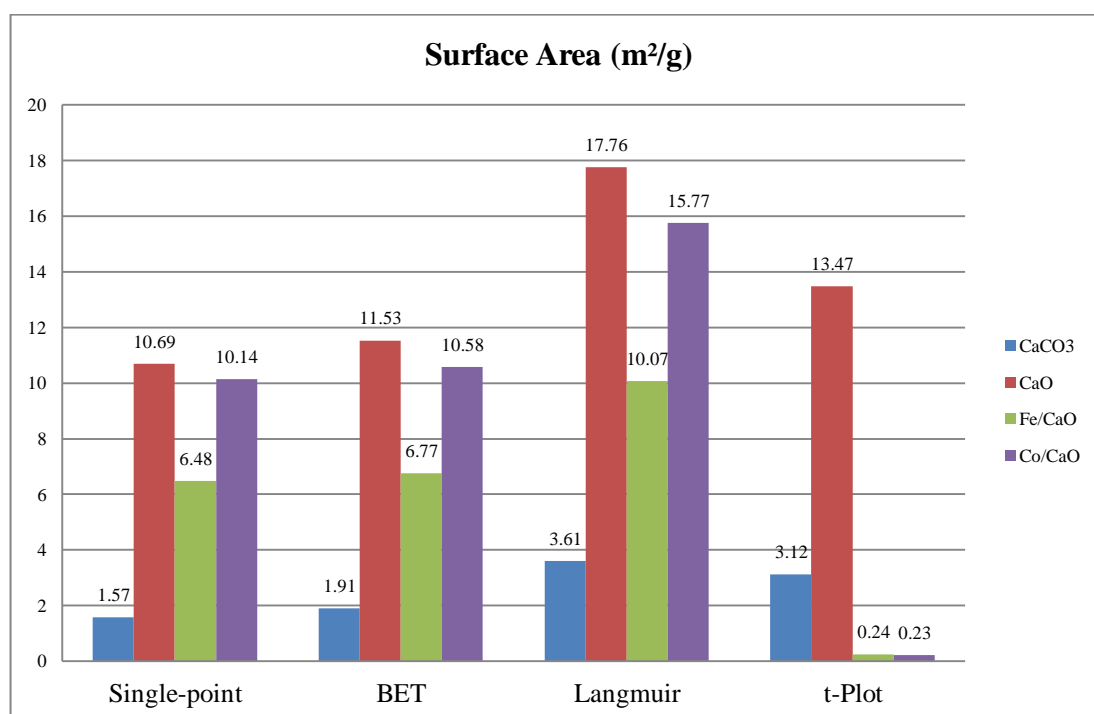
Figure 4.4: Surface area from various analysis techniques

The analyses of the surface area are divided into four; single point surface area, BET surface area, Langmuir surface area and t-plot surface area.

The single point is based on the specific pressure ratio and the Langmuir surface is indicating the surface area available via single layer adsorption while the BET are more into multi-layer adsorption. The t-plot is for the external area of the catalyst.

From this graph, it can be said that the surface area of the catalyst increase after calcination, while CaO provide the largest surface area of all the samples. The importance of the surface area that it will provide more point in contact with the

metal sites – which are the catalyst reaction will be. From here we could see that the CaO and the Co/CaO provide better surface area as compared to Fe/CaO, in which it may indicate higher point in contact between the metal and the reactant gases during the synthesis.

CaO overall indicate higher surface area, while CaO with metal loading decreases in term of areas. The t-plot for both metal loads have significant lower value than CaO, in which it may indicate the pores are well-developed in these two catalyst that the external surface area are significantly lower than CaO catalyst.

	Pore Volume (cm³/g)				
	SP Adsorption	SP Desorption	t-plot micropore	BJH Adsp. cumulative	BJH Dsrp. cumulative
CaCO3	4.86E-03	4.30E-03	-7.59E-04	5.80E-03	5.98E-03
CaO	6.96E-02	8.12E-02	-1.21E-03	9.30E-02	9.27E-02
Fe/CaO	3.13E-02	3.39E-02	4.50E-05	4.09E-02	4.08E-02
Co/CaO	5.12E-02	6.15E-02	-1.40E-05	6.89E-02	6.88E-02

Table 4.6: Collection of the pore volume data

The following figure 4.5 represents the pore volume of the catalysts based on table 4.6. The pore volumes are calculated by the absorption and desorption of gases bases on single point method and Barret-Joyner-Halenda (BJH) method.
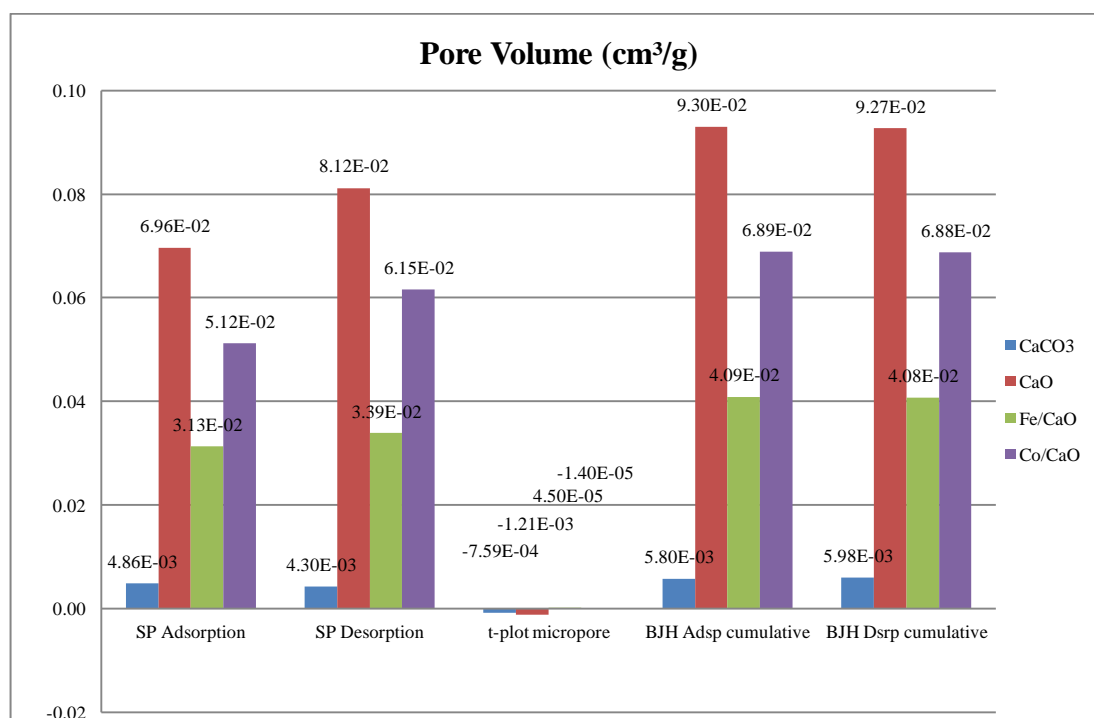
Figure 4.5: Pore volume analysis

From figure 4.5, the data can be seen that the pore volumes of the catalyst increases after the calcination significantly. But as compared to CaO sample, the catalysts with metal loading indicate lower surface volume with respect to CaO sample.

One indication that is worth noting here is the value of the t-plot micropore is negative in value – which are noting that the estimate pore volume over area are indicating small amount of micropore (Marczewski, 2012)

	Pore Size ($\text{Å} = 10^{-10}$m)			
	Adsp avg pore	Dsrp avg pore	BJH Adsp avg	BJH Dsrp avg
CaCO3	101.7	89.9	86.6	93.6
CaO	241.4	281.6	293.0	269.7
Fe/CaO	185.0	200.3	246.6	241.0
Co/CaO	193.7	232.6	256.5	241.4

Table 4.7: Collection of the pore size data

Table 4.7 shows the pore sizes of the catalyst while figure 4.6 gives the visual representation the data. The absorption and desorption pore sizes are based on BET and BJH method.
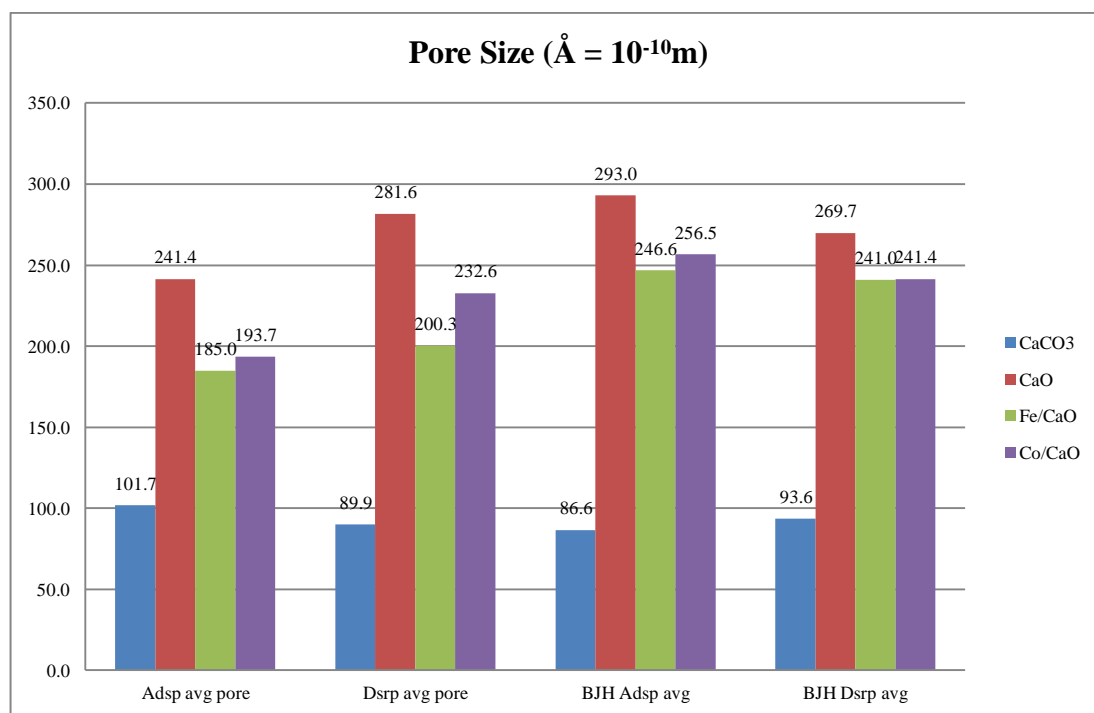
Figure 4.6: Pore size analysis

From figure 4.6, it can be noted that the pore sizes increases after the calcination and the metal-loaded CaO samples provide almost similar pore sizes between both of them. CaO sample provides the largest pore volumes sizes among the three catalysts.

4.4.1 Data analysis (BET)

From the data analysis, it can be observed that the characteristic of the catalysts in term of surface area and sizes increases after the calcination; and CaO samples provides the best surface area and other characteristic as compared to other catalyst samples in term of surface area analyses.

4.5 Temperature Programmed Reaction (TPR/TPO)

The Temperature Programmed Reduction (TPR) and Temperature Programmed Oxidation (TPO) are the analyses to determine the catalyst characteristic in term of activation and the ability of the catalyst to regenerate over the temperature profile.

It can also be used to properly determine the components existed in the catalyst when the reduction is occurred.

4.5.1 CaO sample

4.5.1.1 TPR
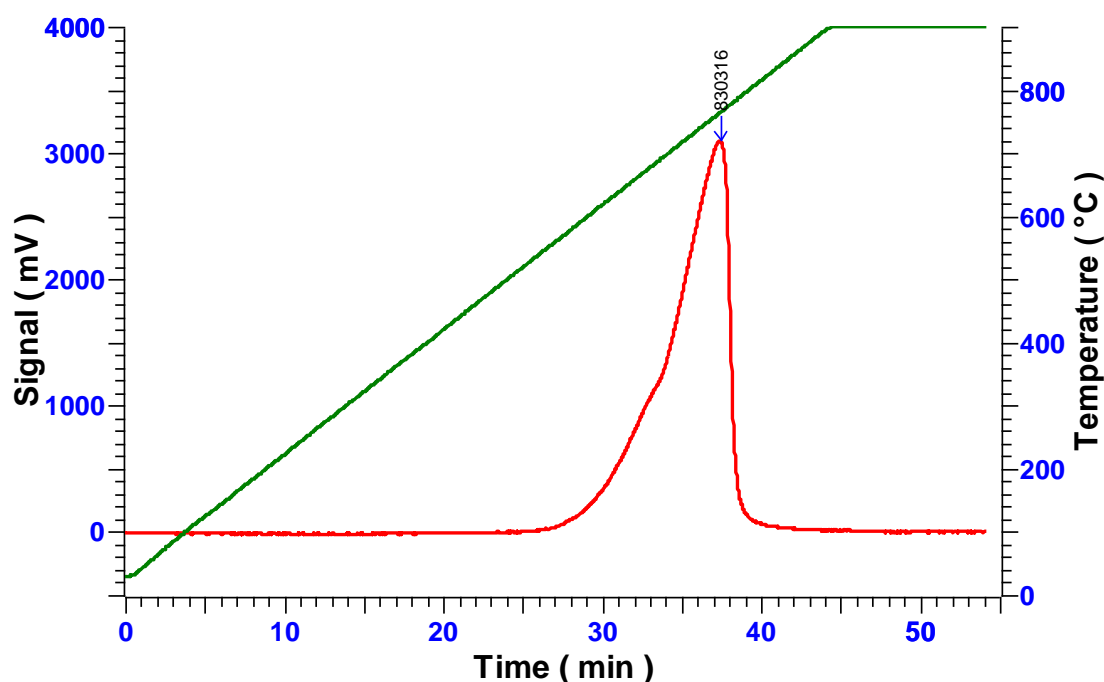
Figure 4.7: TPR result for CaO sample

The sample is run under 5% hydrogen under the period of time. From the peak indicate the hydrogen consumption of the sample to be properly reduced to metal by the following equation:

$$CaO + H_2 \rightarrow Ca + H_2O$$
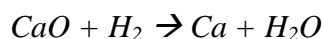
The result gave the amount of the gas absorbed during the analysis based on the integral of the peak area. The amount of gas absorbed is 654.10097μmol/g.

4.5.1.2 TPO
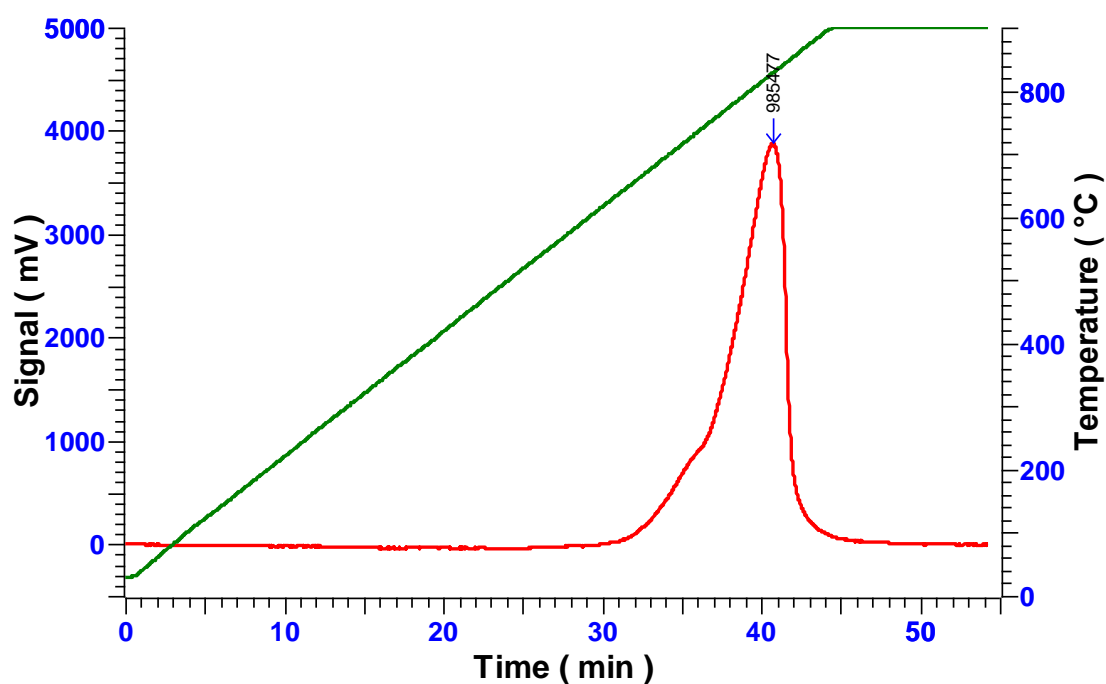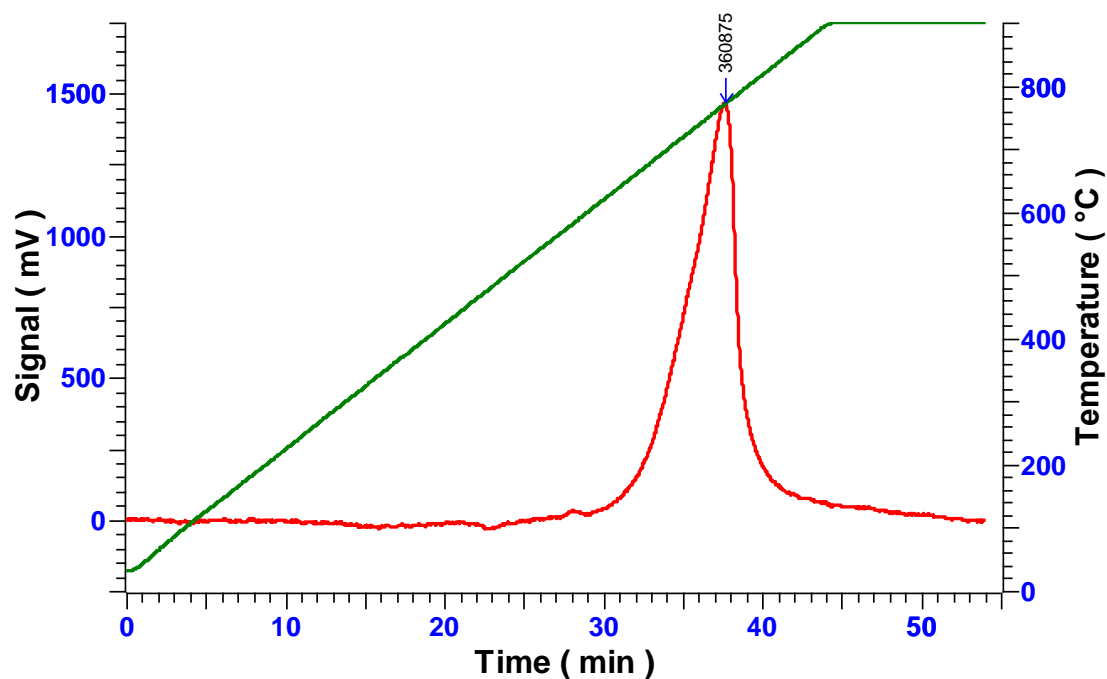

Figure 4.8: TPO result for CaO sample

Figure 4.8 shows the oxidation curve of the CaO sample, in which the sample shows a single peak. The TPO indicate the catalyst can be oxidized over 5% oxygen gas mixture to regenerate the catalyst again. However, as the oxidation is not yet calibrated, the amount of gas absorbed cannot be obtained.
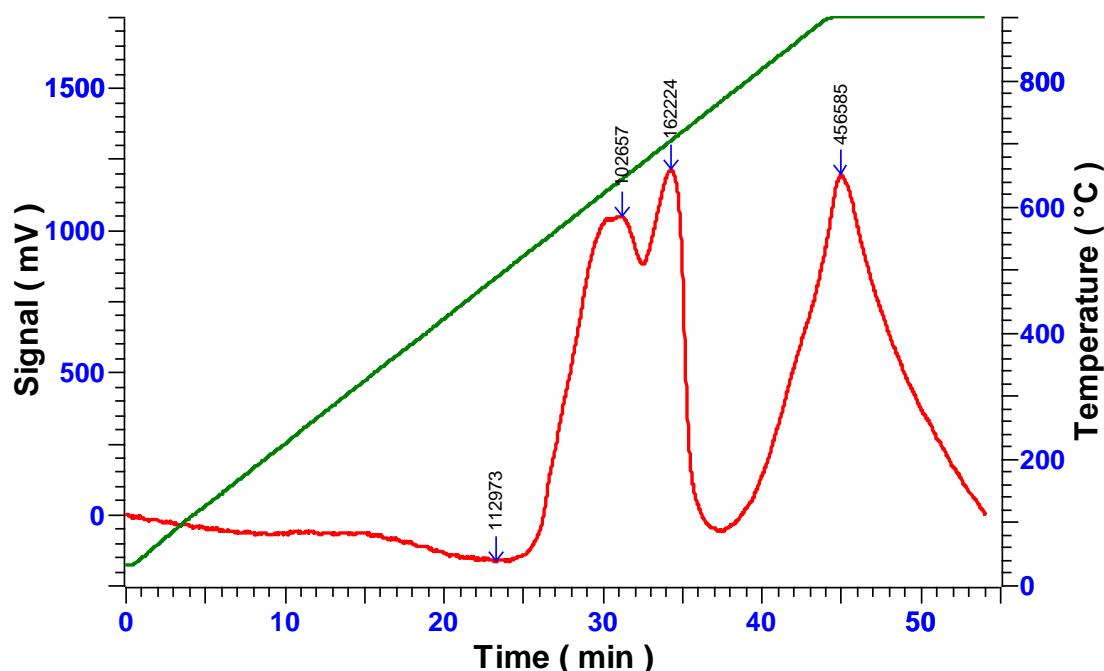
4.5.2   Fe/CaO sample

4.5.2.1   TPR
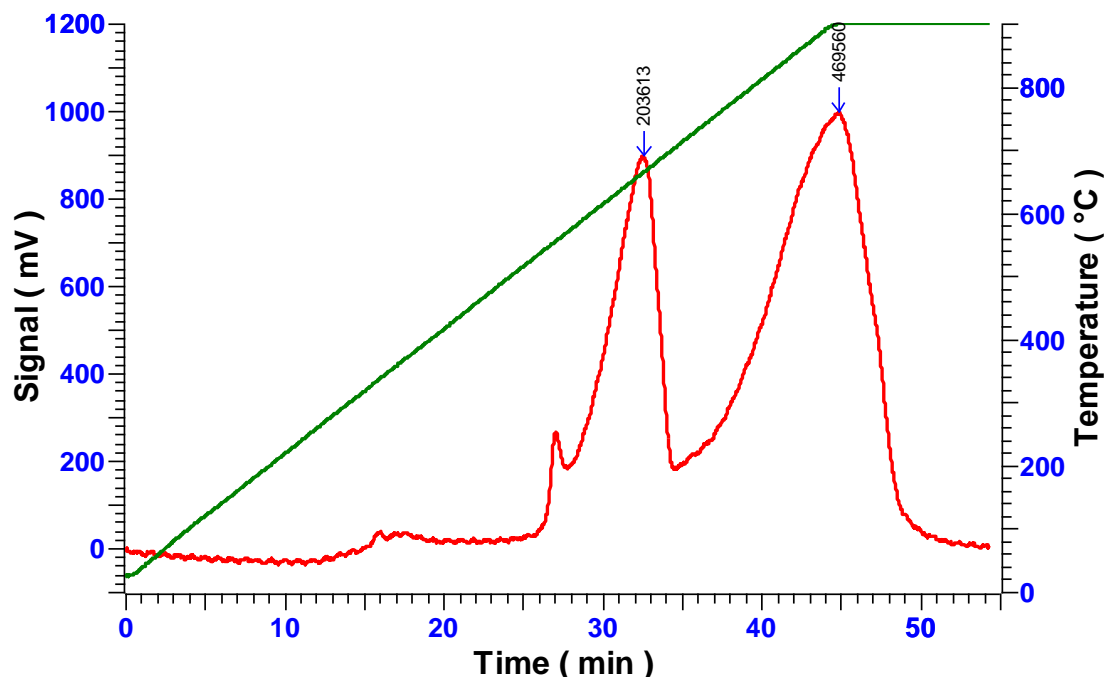
Figure 4.9: TPR result for Fe/CaO sample

The sample is run over 5% hydrogen gas mixtures under certain period of time over the range to 1173K. The peaks indicate the hydrogen consumption and the reduction processes of the sample. The theoretical assumption is that the sample is in form of oxide and there are two oxides present; calcium oxide and iron (III) oxide.

The reduction equations are as follows:

$$CaO + H_2 \rightarrow Ca + H_2O$$
$$Fe_2O_3 + 3H_2 \rightarrow 2Fe + 3H_2O$$
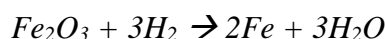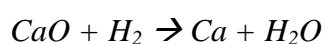
But, as the XRD shows the presence of carbon over the catalyst, it can be assumed that there is also some deposition of carbon over the catalyst via the following equation:

$$CO_3^- + 3H_2 \rightarrow C + 3H_2O$$
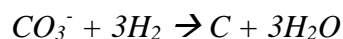
The amount of the gas absorbed over the Fe/CaO sample is 618.69234μmol/g.

4.5.2.2 TPO
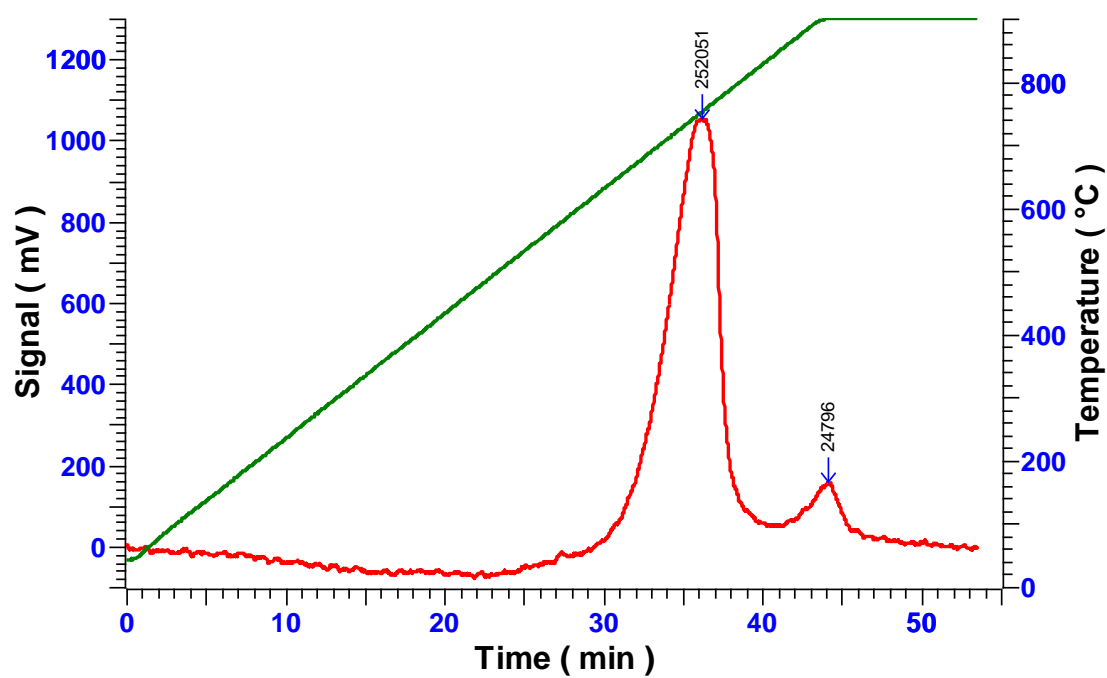

Figure 4.10: TPO result for Fe/CaO sample

Figure 4.10 shows the oxidation curve of the Fe/CaO sample, in which the sample shows a single peak. The TPO indicate the catalyst can be oxidized over 5% oxygen gas mixture to regenerate the catalyst again.

4.5.3   Co/CaO sample

4.5.3.1   TPR

Figure 4.11: TPR result for Co/CaO sample

The sample is run over 5% hydrogen gas mixtures under certain period of time over the range to 1173K. The peaks indicate the hydrogen consumption and the reduction processes of the sample. The theoretical assumption is that the sample is in form of oxide and there are two oxides present; calcium oxide and cobalt (II) oxide.

The reduction equations are as follows:

$$CaO + H_2 \rightarrow Ca + H_2O$$
$$CoO + H_2 \rightarrow Co + H_2O$$
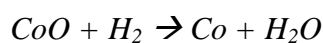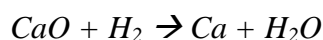
Since the XRD of the sample shows a residue of sulphate, it can be assumed that there is deposition of sulphur and sulphur oxides on the catalyst surface – as well as deposition of carbon from the carbonate ion. For theoretical argumentation, it is assumed the sulphur is completely reduced under over the time.

$$SO_4^{2-} + 4H_2 \rightarrow S + 4H_2O$$
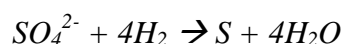
The amount of the gas absorbed over the Co/CaO sample is 862.19372μmol/g.

24

4.5.3.2 TPO

Figure 4.12: TPO result for Co/CaO sample

Figure 4.12 shows the oxidation curve of the Co/CaO sample, in which the sample shows double peaks. This might indicate the oxidation over the catalyst surface took on two components.

4.6 Surface morphology and metal deposition on catalysts' surface

4.6.1 Transmission Electron Microscopy (TEM)

The catalyst samples are prepared by diluting them in iso-propanol solution to segregate the compounds. The samples are then put into the support mesh which are then used under the microscope

4.6.1.1 CaO
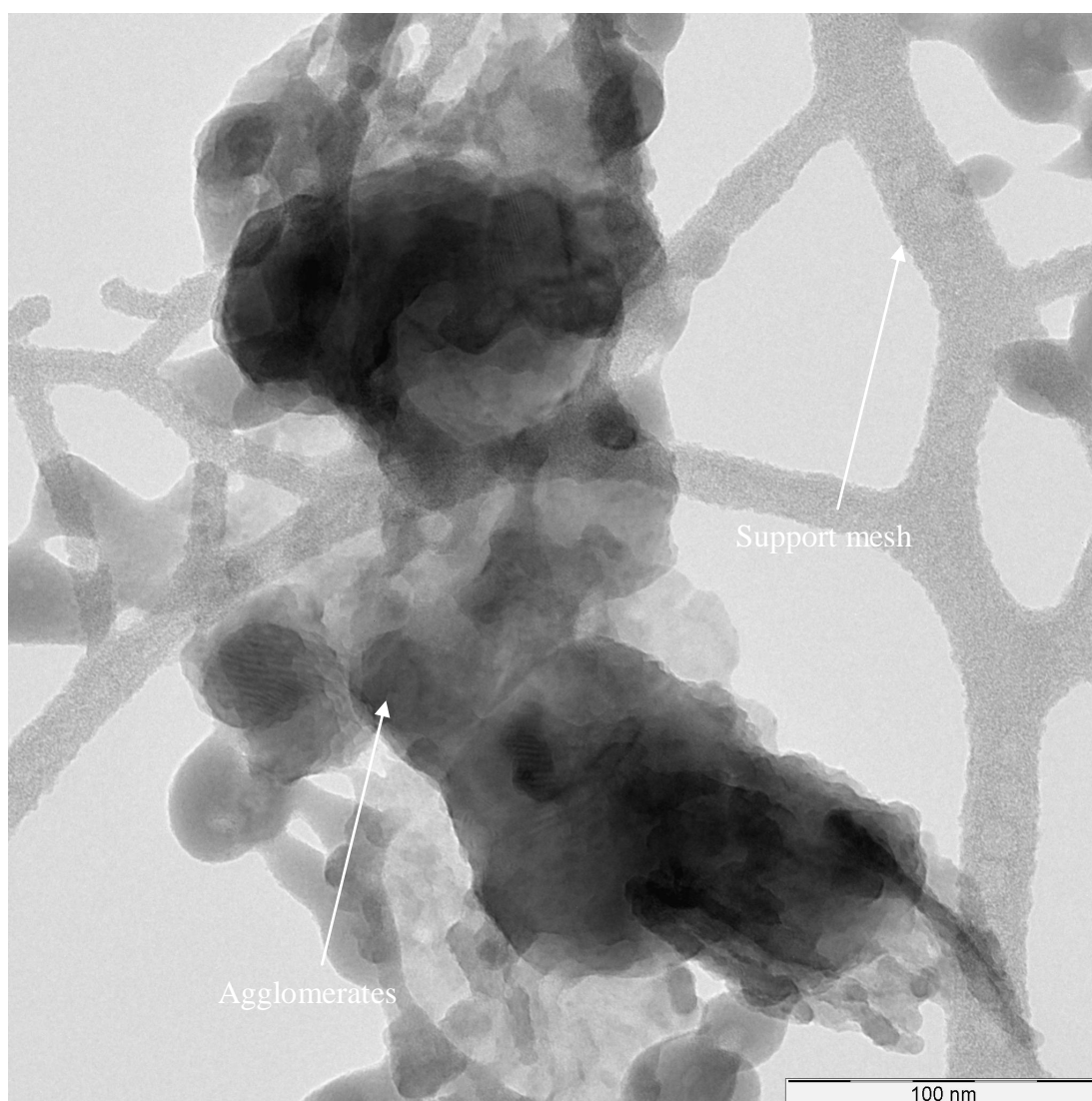
Figure 4.13: 100nm scale CaO

Figure 4.13 shows the CaO sample attached on the holder. The agglomerates are showing the basic structure of the CaO catalyst. The fringes on the picture are usually the active metal sites available on the catalyst.

26
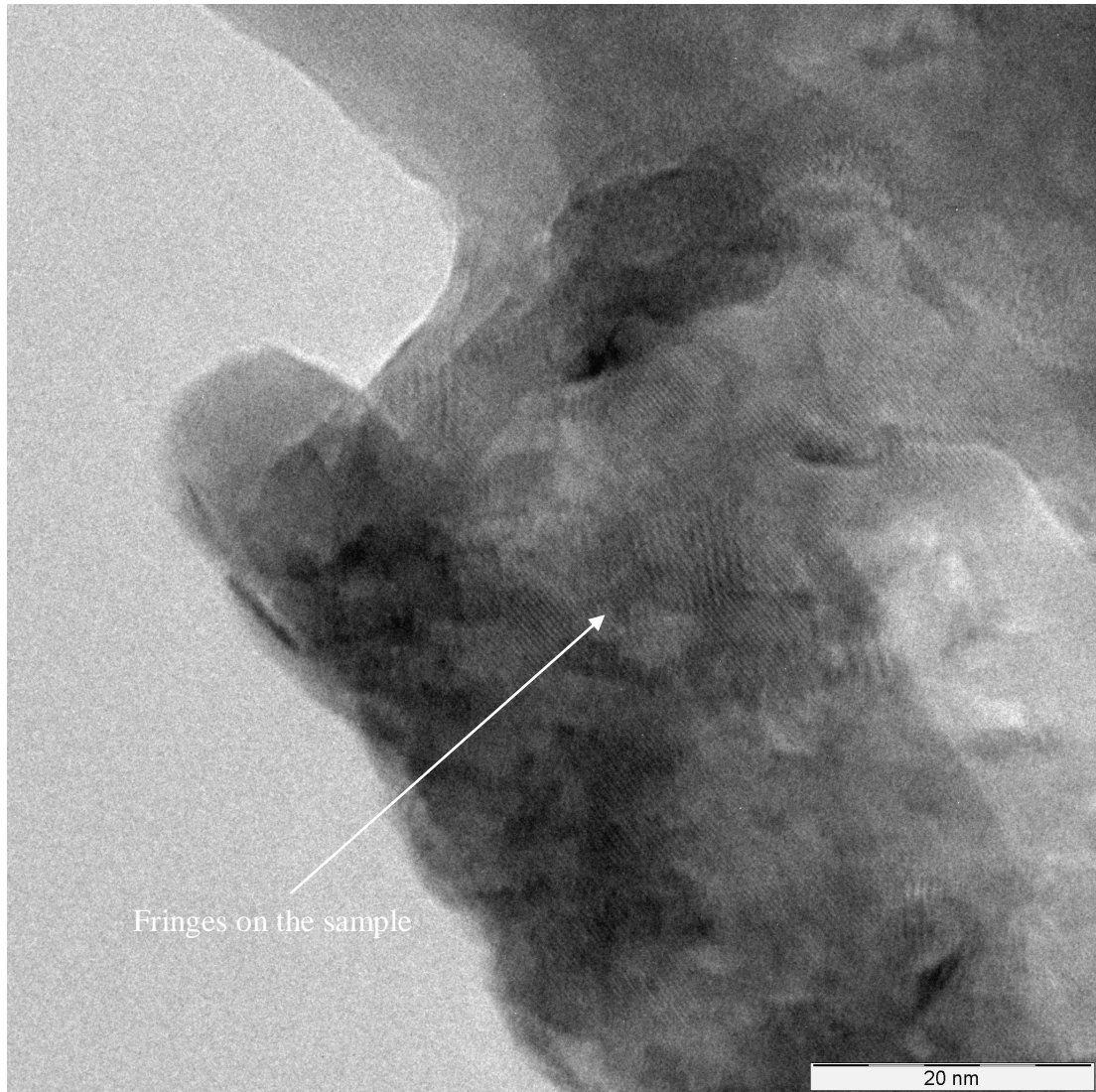
Figure 4.14: 20nm scale CaO

In figure 4.14, the sample is magnified and the fringes are easier to see now.

4.6.1.2 Fe/CaO
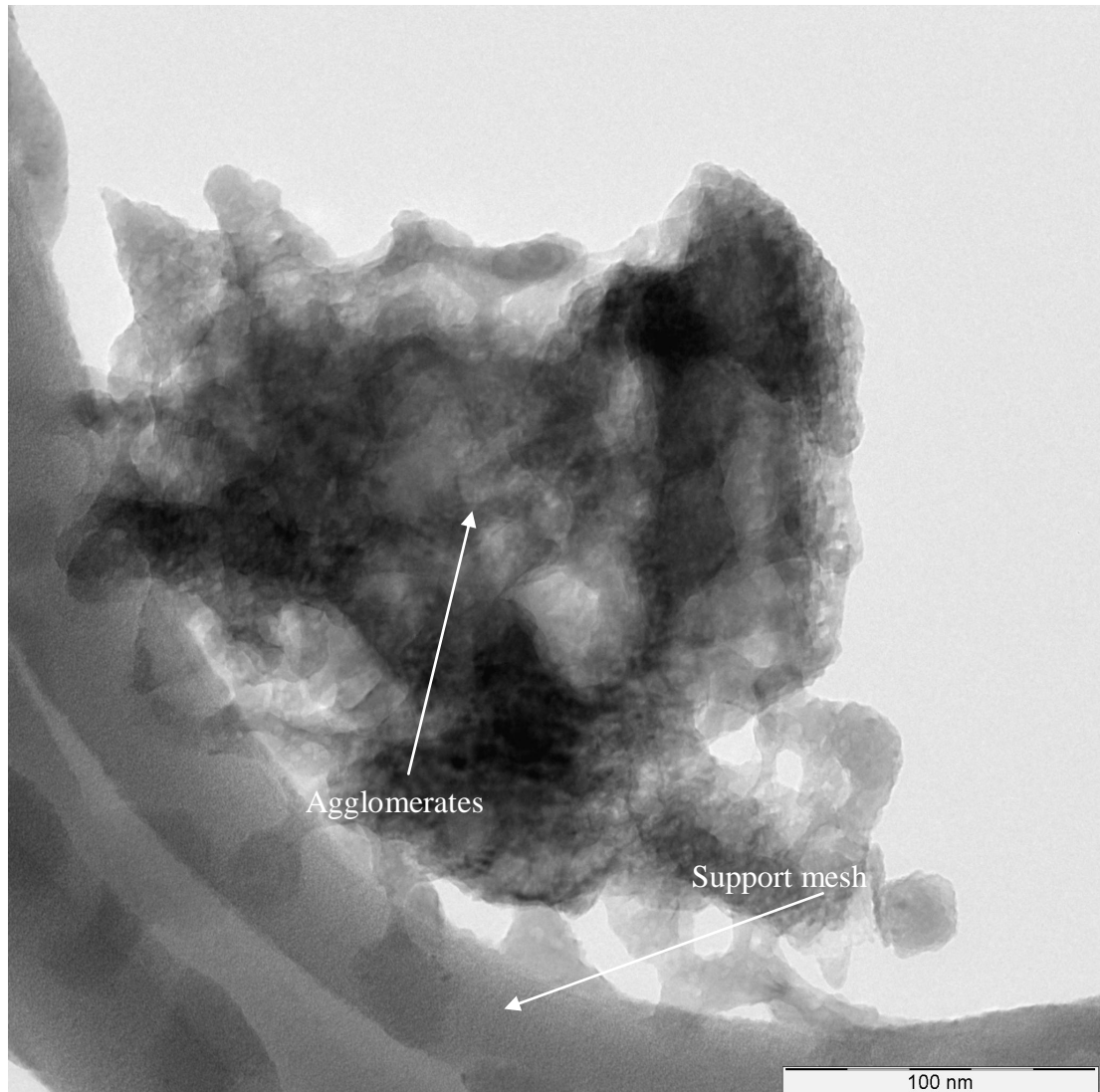
Figure 4.15: 100nm scale Fe/CaO sample

Figure 4.15 shows the Fe/CaO samples on 100nm scale. The agglomerates are clustered together tightly that the electron cannot pass through easily, which are then resembled by the dark tonal area of the agglomerates.
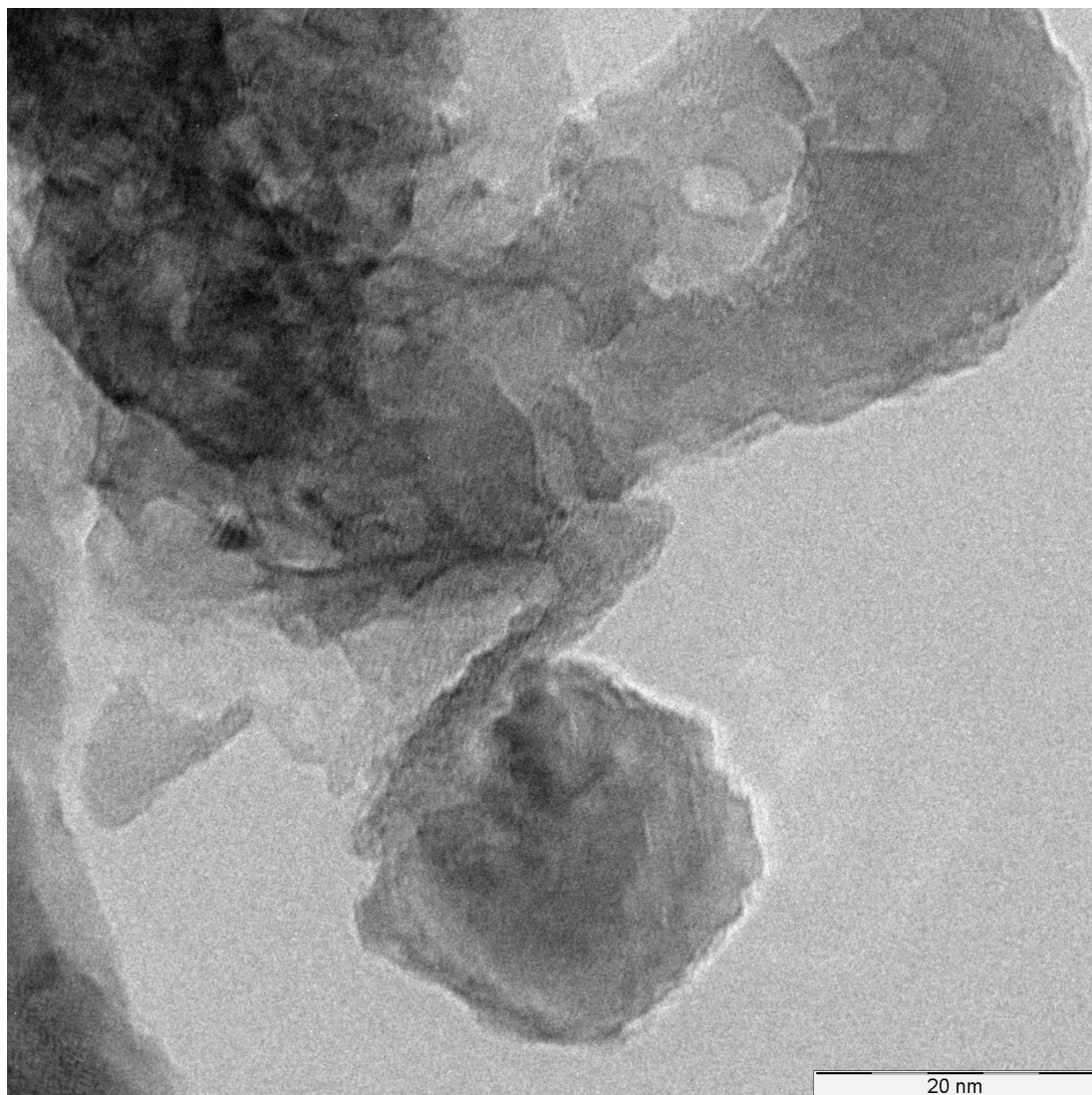
Figure 4.16: 20nm scale Fe/CaO sample

Figure 4.16 shows the larger magnification over some part of the catalyst. Fringes are not overly visible but are present.
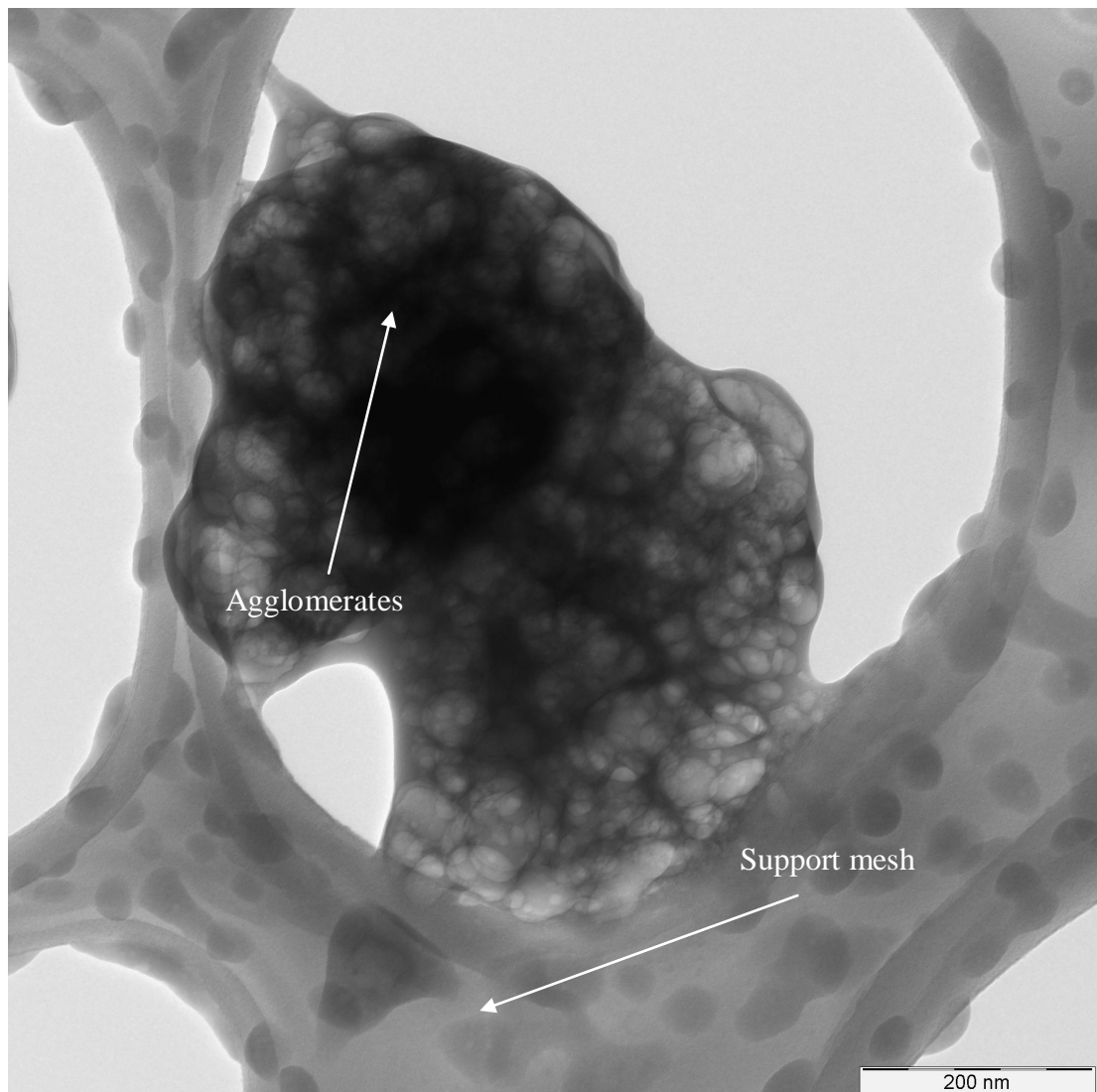
4.6.1.3   Co/CaO

Figure 4.17: 200nm scale Co/CaO sample

Figure 4.17 shows the agglomerates of Co/CaO sample. The sample are overly clustered that the catalyst are not really visible. The fringes are hardly can be seen here.
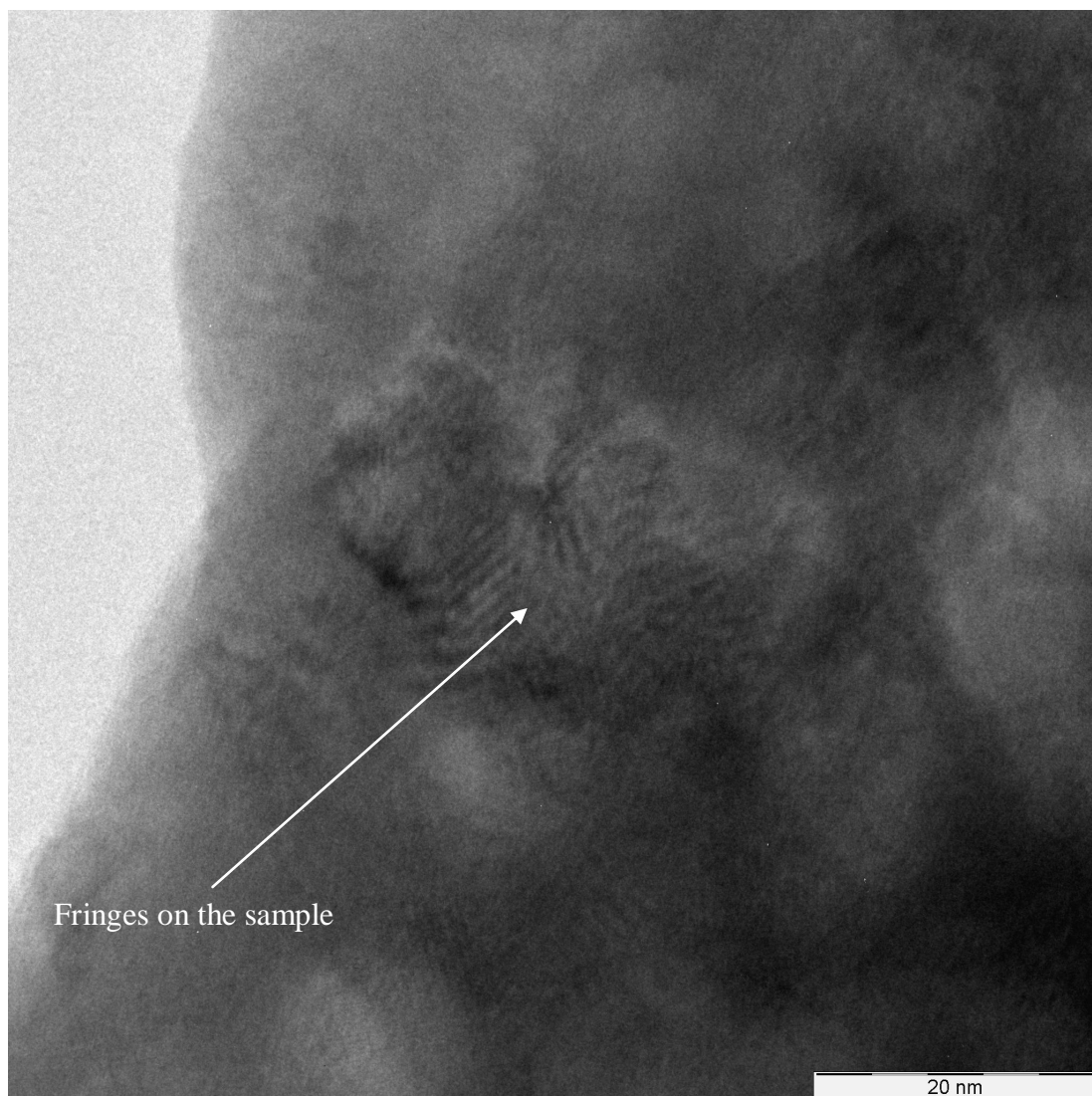
Figure 4.18: 20nm scale Co/CaO sample

Figure 4.18 shows the Co/CaO sample on higher magnification. The fringes are visible here although the agglomerates are big in nature.

The TEM analysis provides the atomic-scale analysis of the catalyst component. The pictures are scaled from range of 200nm to 20nm. The dark parts of the catalyst are being said to be larger than nanoparticle sizes. However, in the 20nm scale pictures the metal site can be seen from the fringes available from the surface. This usually indicates the presence of metal site on the catalyst surface.

To confirm with the metal site on the catalyst support, FESEM will be conducted to see the metal dispersion and surface morphology of the catalyst samples.

4.6.2 Field Emission Scanning Electron Microscope (FESEM)
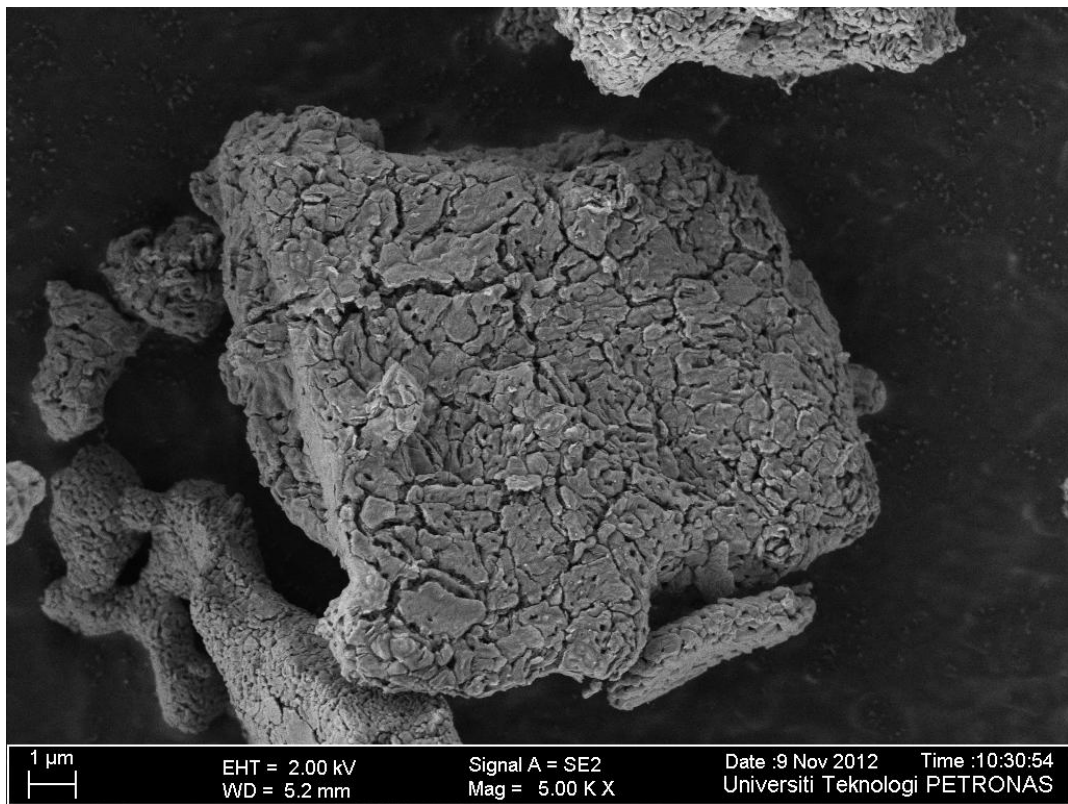
4.6.2.1 CaO

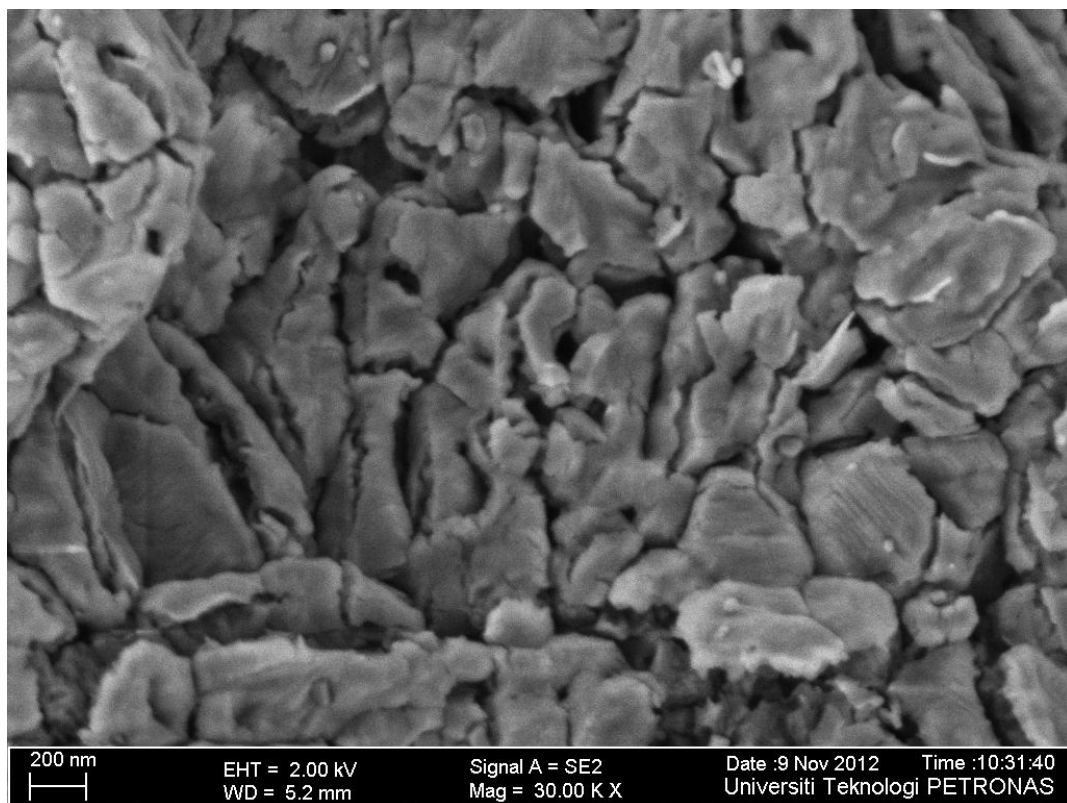Figure 4.19: CaO sample on 5.00K magnification

Figure 4.20: CaO sample on 30.00K magnification

Figure 4.19 shows the CaO sample on 5.00K magnification. The pores and the surface morphology can be visibly seen here in the magnification.

While in figure 4.20 shows the magnification on 30.00K, where the surface of the catalyst can be seen clearly as well as the pores available on the surface.
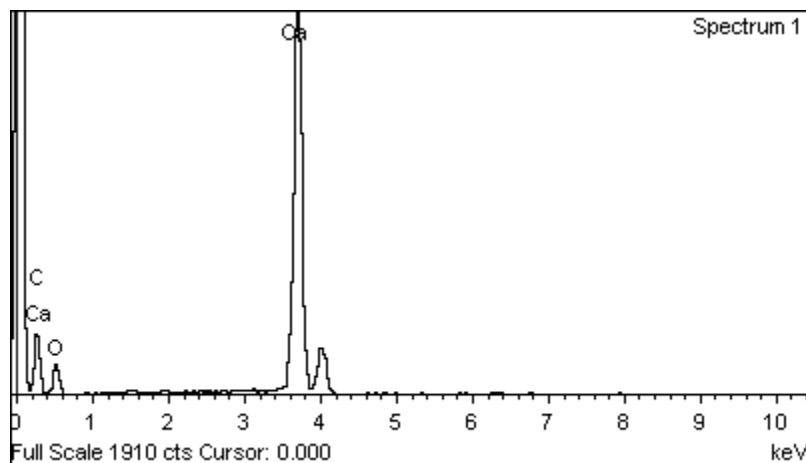

Figure 4.21: EDX analysis of CaO sample

Element	Weight%	Atomic%
C K	23.92	39.62
O K	30.27	37.64
Ca K	45.80	22.74

Table 4.8: EDX analysis of CaO sample

The EDX analysis over the sample indicates that there are traces of carbon over the catalyst. This shows that the catalyst is not entirely converted during the calcination period.
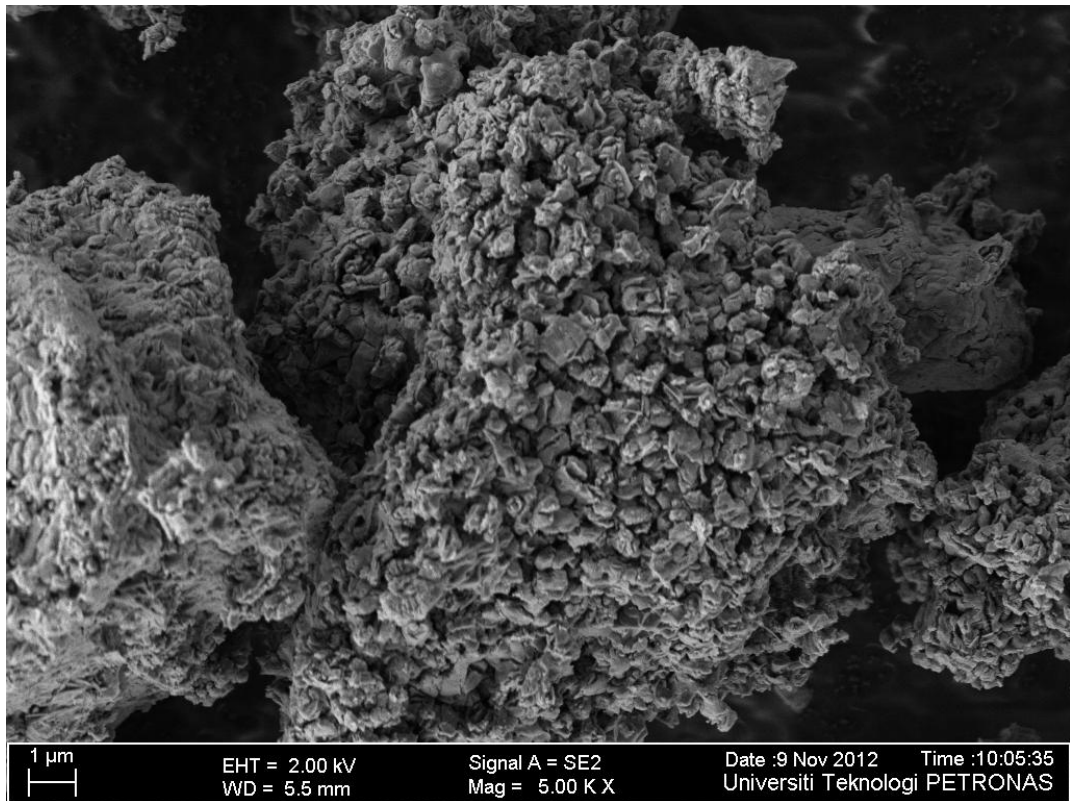
4.6.2.2   Fe/CaO
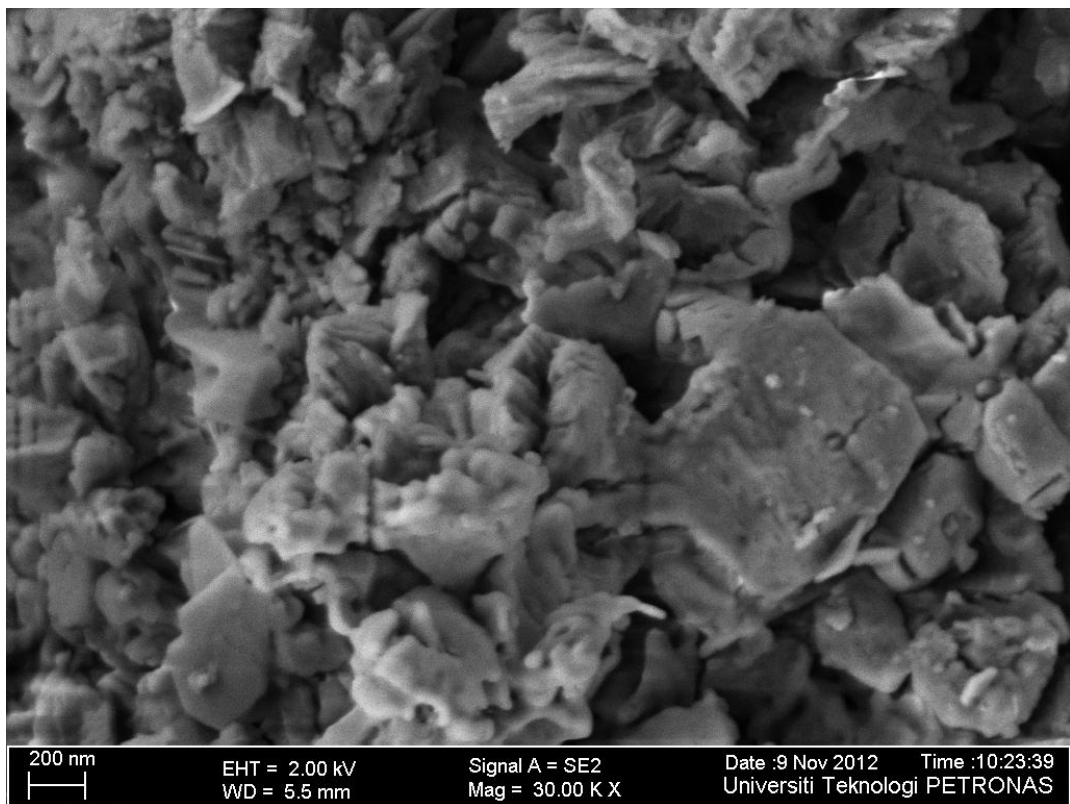

Figure 4.22: Fe/CaO sample on 5.00K magnification

Figure 4.23: Fe/CaO sample on 30.00K magnification

Figure 4.22 shows the Fe/CaO sample on 5.00K magnification. The pores and the surface morphology can be visibly seen here in the magnification. The structure and the surface of the catalyst are completely different as compared to CaO sample, and the pores are comparatively more than CaO sample.

Figure 4.23 shows the magnification on 30.00K. The following figure and table shows the EDX analysis of the Fe/CaO component.
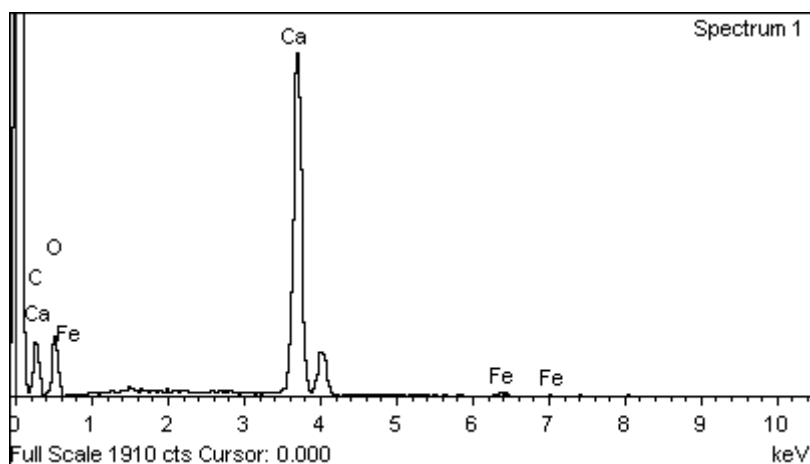

Figure 4.24: EDX analysis of Fe/CaO sample

Element	Weight%	Atomic%
C K	20.19	31.97
O K	42.44	50.44
Ca K	36.39	17.26
Fe K	0.97	0.33

Table 4.9: EDX analysis for Fe/CaO sample

The EDX analysis provides indicates the percent of component over the selected area. The presence of carbon indicates the calcium are not calcined thoroughly during the calcination period.
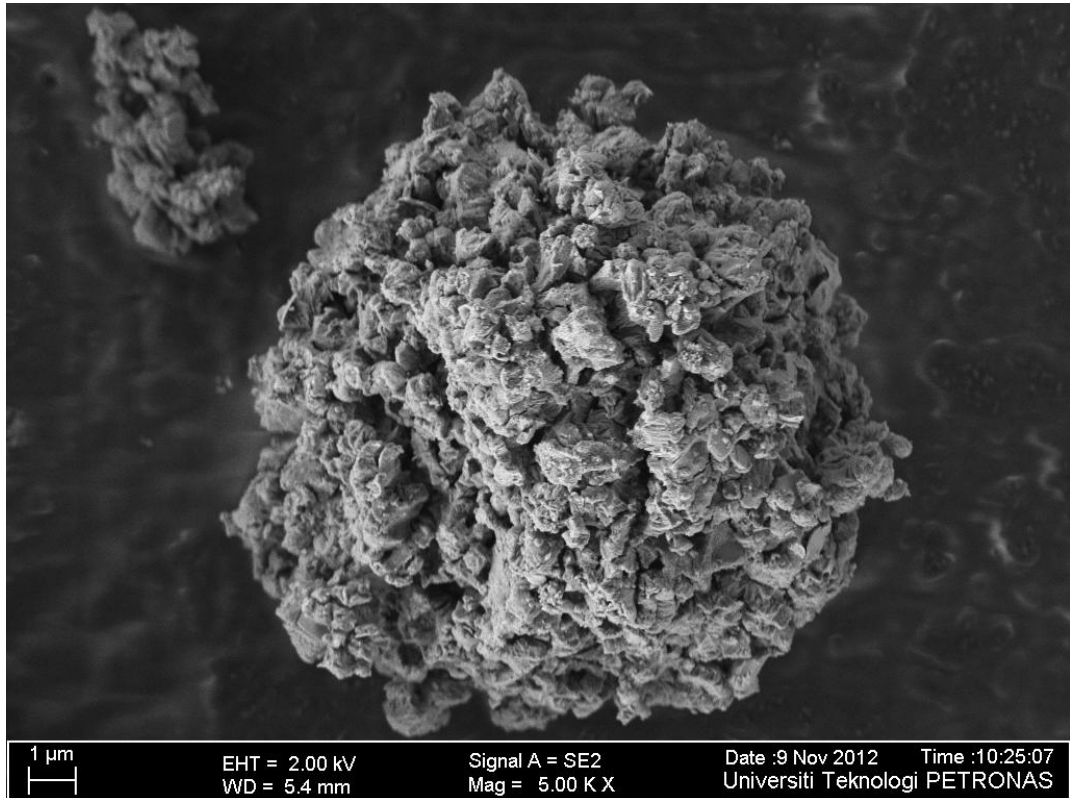
4.6.2.3   Co/CaO

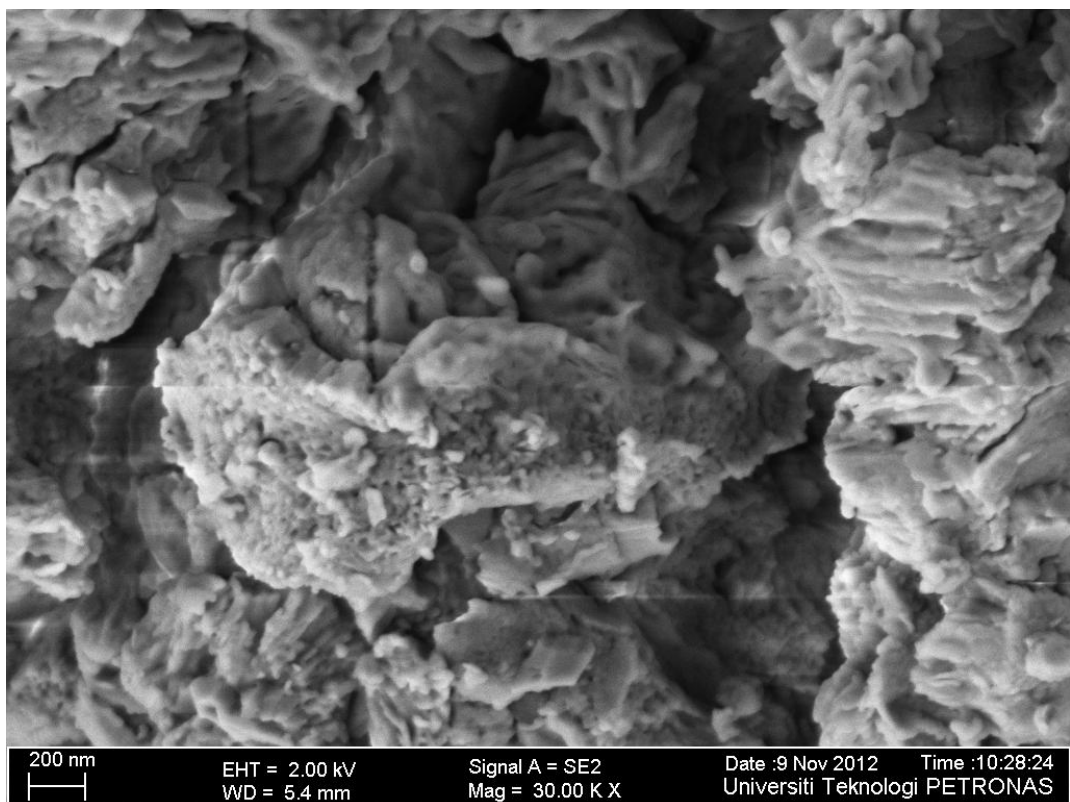
Figure 4.25: Co/CaO sample on 5.00K magnification

Figure 4.26: Co/CaO on 30.00K magnification

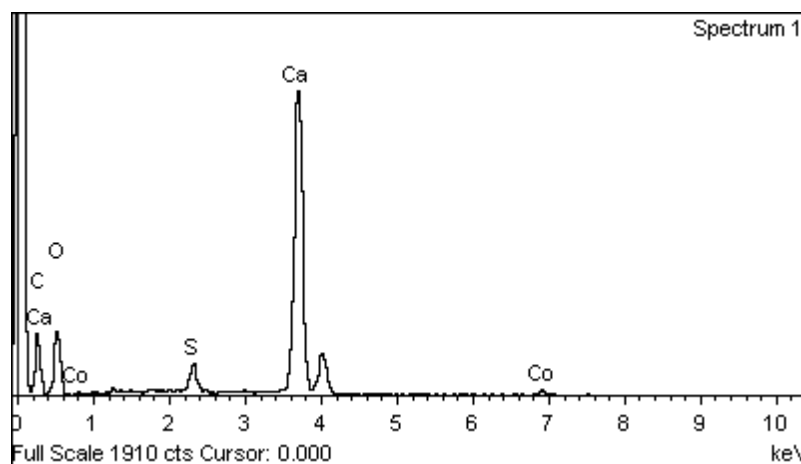The figures show the catalyst surface morphology of Co/CaO sample.

Figure 4.27: EDX analysis of Co/CaO sample

Element	Weight%	Atomic%
C K	23.66	36.19
O K	41.78	47.97
S K	1.83	1.05
Ca K	31.32	14.36
Co K	1.40	0.44

Table 4.10: EDX analysis of Co/CaO sample

There are traces of sulphur from the sulphate ions left from the catalyst preparation indicated from the EDX analysis. Traces of carbon is also detected which indicate the calcination of the sample are not completely reduced to theoretical reduction over the calcination method.

5 Recommendation and Conclusion

5.2 Conclusion

From the analyses, the basic properties of the catalyst can be obtained to indicate the procedures and preparation of the catalyst are as par as the expectation.

The CaO sample currently gives the best overall characteristic as compares to other two catalyst sample while the Co/CaO sample are indicated to be contaminated with sulphur compound from the preparation.

The catalyst kinetics can only be obtained through FTS reaction to see the possibility of calcium as the catalyst support. The objective and scopes of the topic are achieved.

5.3 Recommendations

i. The Co/CaO catalyst must be re-prepared from cobalt nitrate solution to prevent sulphur contamination of the catalyst.

ii. The nanocatalyst preparation method can be used as catalyst preparation to enable TEM analysis to be clearly visible.

iii. The catalyst to run in FTS for over 10 hours or more to provide the insight of the catalyst kinetic as well as conversion of syngas over the catalyst.

6   References

1. Stranges, A.N. (2007), A History of the Fischer-Tropsch Synthesis in Germany 1926-45, Fischer-Tropsch Synthesis, Catalysts and Catalysis 163, B.H. Davis and M. L. Occelli (Editors), Elsevier B.V.
2. Hoek, A. (2006), The Shell GTL Process: Towards a World Scale Project in Qatar: the Pearl Project, presentation slides retrieved from
   http://www.dgmk.de/petrochemistry/abstracts_content14/Hoek.pdf
3. Rapier, R. (2010), Inside Shell's Bintulu GTL Plant, Consumer Energy Report, retrieved from
   http://www.consumerenergyreport.com/2010/11/14/inside-shells-bintulu-gtl-plant/
4. HubPages, What is Fischer-Tropsch Process?, retrieved on 18 June 2012
   http://flyingvet.hubpages.com/hub/Fischer-Tropsch-process
5. Tan, B.K., (2002), Environmental Geology of Limestone in Malaysia, Universiti Kebangsaan Malaysia, Faculty of Science and Technology, Geology Programme, retrieved from
   http://www.karst.edu.cn/igcp/igcp448/2002/3-2-7.pdf
6. Cheney Lime & Cement Company, retrieved from
   http://www.cheneylime.com/chemist.htm
7. Dry, M. E. (2004), FT Catalyst, Fischer-Tropsch Technology, Studies in Surface Sciences and Catalysis 152, A. Steynberg and M. Dry (Editors), Elsevier B.V.
8. Dry, M. E (2002), Catalysis Today 71, Elsevier B.V
9. May, J. (2002), The Fischer-Tropsch Process and Its Influence, slides retrieved from
   http://stoltz.caltech.edu/litmtg/2002/may-lit-9_26_02.pdf
10. Marczewski (2002), A Practical Guide to Isotherms of ADSORPTION on Heterogeneous Surfaces, retrieved on 01-12-2012 from
    http://adsorption.org/awm/ads/t-plot.htm
11. May J. (2002), The Fischer-Tropsch process and its Influence
12. Luo and Davis (2002), Fischer-Tropsch synthesis: Group II alkali-earth metal promoted catalysts, Applied Catalyst A: General 246(2003), page 171-181
13. Motchelaho, Anne (2011), Iron and cobalt catalysts supported on carbon nanotubes for the use in Fischer-Tropsch synthesis, University of Witwatersrand, Johannesburg
14. Yao, Yali (2011), Fischer-Tropsch synthesis using CO_2-containing syngas mixtures over cobalt and iron based catalysts, University of Witwatersrand, Johannesburg

The calculation for the decomposition ratio:

$CaCO_3$	100.09 g/mol	CaO	56.08 g/mol

Decomposition ratio:

$$\frac{CaO}{CaCO_3} = \frac{56.08 \; g/mol}{100.09 \; g/mol} = 0.5603 \; (TGA: 0.5518)$$

$Fe(NO)_3.9H_2O$	404 g/mol	Fe_2O_3	159.69 g/mol

Decomposition ratio:

$$\frac{Fe_2O_3}{Fe(NO)_3.9H_2O} = \frac{159.69 \; g/mol}{404 \; g/mol} = 0.3953$$

$CoSO_4.H_2O$	173.01 g/mol	CoO	74.93 g/mol

Decomposition ratio:

$$\frac{CoO}{CoSO_4.H_2O} = \frac{173.01 \; g/mol}{74.93 \; g/mol} = 0.4331$$